Soft-matter Artificial Muscle
by Electrochemical Surface Oxidation of Liquid Metal

Thesis by

Jiahe Liao

Submitted to the Robotics Institute

in partial fulfillment of the requirements for the degree of

Master of Science in Robotics

at

Carnegie Mellon University

Thesis Committee:

Professor Carmel Majidi, Chair
Professor Matthew Travers
Eric Markvicka, Ph.D.

August 2018

Soft-matter Artificial Muscle by Electrochemical Surface Oxidation of Liquid Metal

Jiahe Liao

The Robotics Institute
Carnegie Mellon University

Professor Carmel Majidi, Chair

Abstract

Natural muscles, a result of more than 500 millions years of evolution, are elegant machines that generate force and motion electrochemically. The brief history of robotics does not have the luxury of millions of years to reverse-engineer many aspects of life. The development of artificial muscles therefore seeks to build more muscle-like actuators for robots. Recent advances in the engineering of soft materials have led to the exploration of new paradigms for building artificial muscles from matters that share similar properties with biological tissues. A diversity of physical phenomena has also been used to drive an actuator. Among those are the control of the surface energy of a liquid metal, which often has a significant surface tension which becomes predominant at very small (~mm and ~μm) scales. This work formulates a paradigm for building artificial muscles that utilizes eutectic gallium-indium (EGaIn), a liquid metal alloy (melting point ~15.5 °C) which has a very large surface tension (~624 mN/m) in the absence of surface gallium oxide (Ga_2O_3), as an active material and demonstrates key points in the realization a new class of artificial muscles based on the remarkable controllability of surface tension by electrocapillarity and surface oxidation with small voltages (~1 V). Two different form factors are demonstrated. First, a hybrid structure of coil spring and EGaIn that is capable of contraction in an aqueous sodium hydroxide (NaOH) solution is modeled and experimentally characterized. Second, a core-shell hybrid of EGaIn and polyacrylamide-potassium-hydroxide (PAAm-KOH) hydrogel as an equivalent device is hypothesized and validated. Limitations and issues are discussed. A broader perspective is also provided on the role and uniqueness of this artificial muscle paradigm in the current robotics landscape.

Acknowledgements

I am deeply grateful to Prof. Carmel Majidi for his continual guidance and support.

It has been a privilege to work with and learn from my previous and current lab mates. In particular, I would like to acknowledge Dr. Eric Markvicka for his kind encouragement and support, Dr. Alexi Charalambides for his sharing of experience during my first year, Hesham Zaini for our countless all-nighters, and finally Yun-Sik Ohm for our inspiring collaboration.

Finally, I wish to thank my family for their love and my friends Yan-Jen Huang and Ashwin Khadke for their infinite support.

Contents

List of Figures

List of Tables

Chapter 1

Introduction

This work presents a paradigm for building artificial muscles from liquids and gels that can generate force and motion electrochemically. In Nature, muscles are elegant machines that, when activated by electrical impulses in the nervous system, produce force with chemical energy. The need for more muscle-like function in robots has motivated the recent advances in soft actuators based on a wide range of materials and physical principles [131, 48]. An analogy between the natural and the artificial muscles is shown in Figure 1.1.

The quest for life-like machines has been propelling researchers in robotics to reverse-engineer any aspect of life. This includes the abilities to see [68], to learn [91, 92], to think [111], to move [128, 109, 126, 22], to grow [29], to heal [85, 118], and to evolve [17, 16]. From an evolutionary standpoint, the mobility – the ability of a being to move voluntarily – has been of particular importance for many living organisms to function since the genesis of *Haootia quadriformis*, one of the earliest animal species (~ 560 million years ago) known to show fossil evidence of muscle fibers [77]. Similarly, artificial *muscles* are necessary for a robot to move or manipulate like animals.

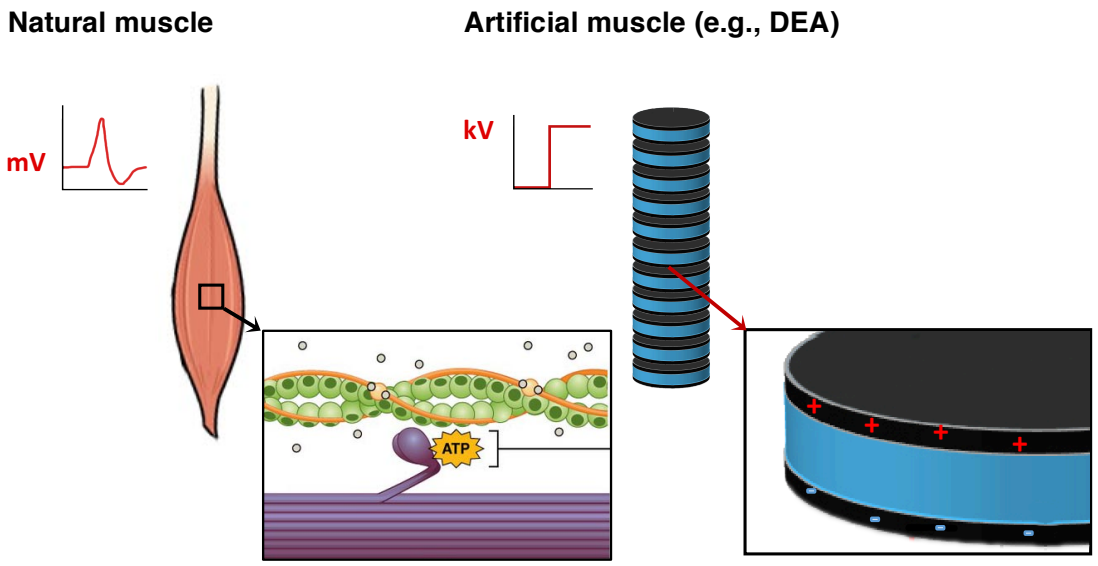

Figure 1.1: Illustration of natural and artificial muscles as stimuli-responsive machines that transform some form of energy into mechanical work. A dielectric elastomer actuator (DEA) is used as an example of artificial muscles.

In the brief history of robotics that merely spans a few decades, in contrast with millions of years of biological evolution, robots are, like most machines, actuated mainly by conventional electromagnetic rotary motors or hydraulics that are made of rigid materials, which limit their mechanical compliance and adaptability to external environment [80]. Another drawback of electric motors as robotic actuators is that their power output is maximized at higher speeds and thus they often need to be geared down for use [93] unless introducing a direct-drive, transmission-free mechanism [4, 5], both of which introduces extra components, weight, and energy loss unlike their biological counterpart. For small-scale robots like micromechanical flying insects (MFI), it is often infeasible to scale down electric motors and gears due to lower power efficiency and higher friction as the size decreases [127]. These all have motivated recent research in new generations of muscle-like actuators.

A key aspect of the development of artificial muscles is the engineering of soft matters, including liquids, colloids, gels, polymers and liquid crystals. These intrinsically soft materials that exhibit elastic and/or viscous characteristics, are particularly well-suited for building actuators to achieve muscle-like functions for several reasons. First, their high deformability allows for greater force production per unit surface. Second, they can be activated by a variety of stimuli such as electricity, magnetic fields, pressurized fluids, heat, light, and pH [48]. Also, some artificial muscles even outperform their natural counterpart by some metrics. Dielectric elastomer actuators (DEA), for example, feature a very high work density ~ 1,000 J/m^3 [48, 87, 78, 3], compared to 8-40 J/m^3 in natural muscles [87, 79, 52, 89], which implies that, when ignoring the power source, a DEA needs much less mass to output the same work since they have similar densities [78]. Finally, compared to long-established rigid structure of robots, soft-bodied robots built with soft-matter artificial muscles that match the compliance and stiffness of skeletal muscles (shear modulus ~16.13 kPa [26]) will be more capable of human-like or animal-like functions in Nature and, therefore, more suitable for a number of practical applications such as cooperative robots for healthcare, lightweight prosthetics, wearable robots, robots for minimally invasive surgery, robots for pipe inspection, and robots for military reconnaissance [80].

The focus of this work is the actuation of eutectic gallium-indium (EGaIn, Figure 1.2) – an electrically conductive liquid metal alloy (75% gallium and 25% indium by weight, ~ 15.5°C melting point [23]) which has a very large surface tension ~ 624 mJ/m^2 in the absence of oxide *skin* on the surface [23]. When oxidized on the surface, the surface tension of EGaIn drops to near zero, a phenomenon that is reversibly controllable by rapid electrochemical reactions using low voltages (~ 1 V) [60, 25]. This work identifies and demonstrates key points in the realization of a new class of artificial muscles based on electrochemical surface

tension tuning of liquid metals. While the ultimate goal is to create a self-contained *cell* that share more characteristics with muscle cells and can be used as the building block for future robots, what is reported here is a step along the path.

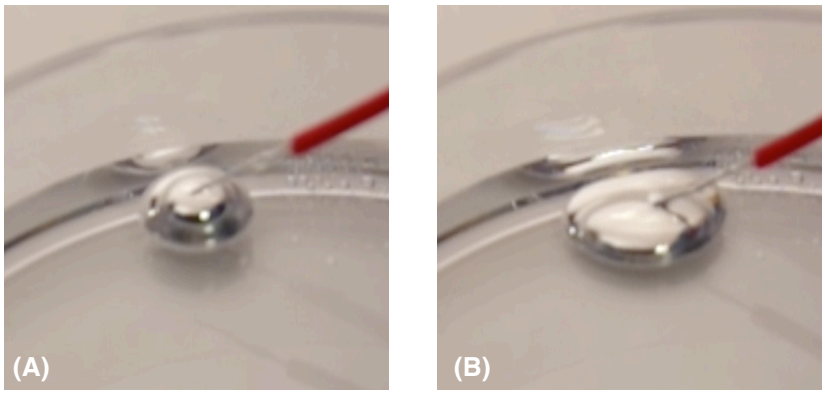

Figure 1.2: Images of a droplet of eutectic gallium-indium (EGaIn) immersed in potassium hydroxide (KOH) solution. (A) The droplet is nearly spherical due to high surface energy. (B) When gallium oxide is formed on the surface, the droplet flattens due to drastically lowered (~ 0) surface tension.

1.1 Muscles in Nature

Biological insight of the principles and performance of natural muscles has been used for the development and benchmarking of artificial muscles. Figure 1.3 presents images of a top-down hierarchy of the muscular system in an animal. A summary of selected properties in this hierarchy is listed in Table 1.1. Unlike most current artificial muscles, a biological muscle is a machine that transforms chemical energy released by ATP hydrolysis into mechanical work.

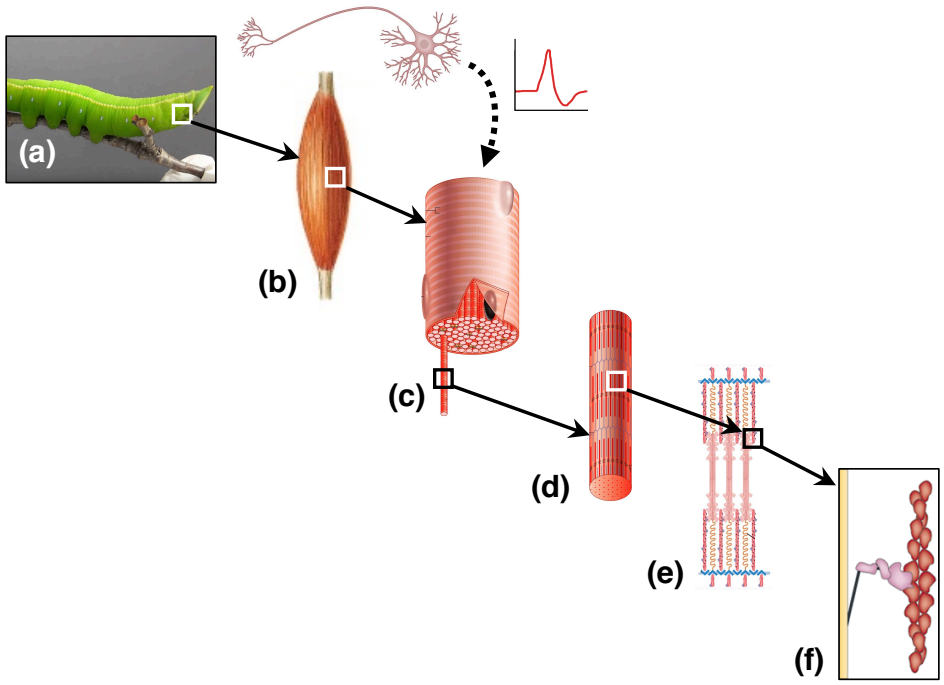

Figure 1.3: Images of the hierarchy of skeletal muscle. (a) Caterpillar (b) Muscle tissue (c) A Muscle cell (muscle fiber) is a basic cellular unit, which is a bundle of even smaller fibers called myofibrils. (d) Myofibril (e) A sarcomere is the basic contractile unit. (f) Actin (thin) and myosin (thick) filaments are responsible for the microscopic sliding and macroscopic contraction of muscles. Titin (elastic) filaments anchor myosins. Image sources: (a) from [81], (b) from [8], (c,d) from [84], (e) from [42], (f) from [114].

Table 1.1: Summary of the hierarchy of mammal skeletal muscles. The shortest muscle in human is the stapedius (~ 1 mm) in the middle ear and the largest is the sartorius (~ 600 mm) along the thigh. The exact length of the longest muscle in blue whales, due to lack of data, is approximated to their whole body length.

Unit	Diameter	Length	Function
Muscle cell (muscle fiber) [52, 103, 44, 12]	• 50 μm (human) • 100 μm (frog)	• 1 – 600 mm (human) • Up to ~ 30 m (blue whale)	Cellular unit. Can function in vitro. Consists of a bundle of myofibrils.
Myofibril [52]	2 μm	(same as above)	Long chain of sarcomeres
Sarcomere [101, 21]	(same as above)	~ 2 μm	Basic contractile unit
Myosin filament [101, 51]	15 nm	~ 1.85 μm	Slide past each other to generate movement
Actin filament [101, 20]	7 nm	~ 1 μm	(same as above)
Titin filament [101, 121]	1 nm	43 nm	Springy protein. Anchor myosin filaments to the end of sarcomere and prevent overstretching.

By the sliding filament theory introduced by Huxley et al. in 1954 [53, 33, 43, 108], the contraction of muscles involves sliding of thin actin filaments past thick myosin filaments inside a sarcomere, where a burst of calcium ions (stimulated by an *action potential* ~ 15 mV at the neuromuscular junction [69, 101]) causes myosin heads to rotate and detach from actin, thereby initiating a *power stroke* (force ~ 2 pN, displacement ~ 10 nm [19, 54, 52, 32, 64]) which shortens the entire sarcomere.

The physical properties (e.g., length scale, density, and elastic modulus) and actuation performance (e.g., strain/stress output, work density, power-to-mass ratio) summarized in Table 1.2 are often a benchmark for comparing artificial muscles. Natural muscles are also characterized by their storage of own energy source (in the form of glycogen) and self-healing, growth and long-term adaptability (i.e., muscle *hypertrophy* or *atrophy*) in response to hyperactivity or inactivity.

1.2 Artificial Muscles for Robots

In this work, an artificial muscle is defined as a synthetic and intrinsically deformable material that, when activated by an external stimulus, consumes power and produces force and motion. The terms *soft actuator* and *artificial muscle* are used interchangeably in this regard.

Modern artificial muscles date back to the 1950s, when J. L. McKibben adapted a pressurized cylindrical bladder for use as an orthotic device [65, 66]. It is capable of linear contraction because any radial expansion in volume is confined by the braided mesh. Originally used as an orthotic appliance for polio patients, it was not until 1955 that the McKibben actuator was patented by Richard H. Gaylord as a standalone pneumatic device [37].

Table 1.2: Properties of skeletal muscles. The length scale of longest mammalian muscle is approximated by the whole body length of blue whales.

Property	Values
Strain output (%) [87, 89, 79]	20 (typical)–40 (max)
Stress output (MPa) [87, 89, 79]	• 0.1–0.35 (human) • 1 (mollusk)
Work density (kJ/m^3) [89]	8 (typical)–40 (max)
Power-to-mass ratio (W/kg) [89]	• 50–284 (human) • 75–309 (humming bird) • 350 (bumble bee) • 14,000 (chameleon tongue) • 36,000–74,000 (froghopper) • 37,600–160,300 (planthopper)
Length scale [103, 44, 12]	• 1 mm–0.6 m (human) • 1 mm–30 m (mammals)
Strain rate (%/s) [87]	500
Density (kg/m^3) [87, 122]	1,037–1,060
Elastic modulus (MPa) [87]	10–60
Efficiency (%) [79, 46]	40
Bandwidth (Hz) [89]	20
Cycle life [87]	10^9

This section presents a comparative overview of the recent advances in artificial muscles that have transformed the landscape of robotics. Among a diversity of actuators, those that are electrically activated are discussed in more details for the following reasons. First, electrical signals are easier to modulate by magnitude, phase, and frequency [48]. Second, actuators that are electrically driven are often significantly more efficient than, for example, those driven by thermal expansion. Finally, these actuators are already compatible and integrable with modern electronic circuitry and hence more suitable for building an untethered autonomous robot [105, 48] than other types of artificial muscles (e.g., pH-activated actuators).

1.2.1 Overview of Soft Actuators

Soft actuators are often categorized by the form of their energy source, as summarized in the following list. It is worth mentioning that this classification is not absolute because some actuators take energy in some form that is, in turn, converted from another form. Joule heating is a typical example, where electrical energy is used to generate thermal energy in many applications such as the heating of shape-memory alloy. Also, some matters like liquid crystals can be activated by different power sources [48].

- Electrical – There are plenty of soft materials that are able to convert electrical energy into mechanical work. *Dielectric elastomer actuators* (DEAs) [140, 67, 100, 87, 3, 58, 59, 57] are an typical example, in which a stack of thin elastomer films (thickness t) sandwiched between conformable electrodes, when applied a voltage on the order of kV, can be compressed by Maxwell stress due to the attraction between opposite charges. The primary weakness of DEAs is the requirement of high voltages, which

cannot be delivered with miniaturized electronics. As another example, *liquid-crystal elastomer* actuators (LCEs) are slightly crosslinked liquid crystal networks which combine the self-organizing property of liquid crystals and the elasticity of elastomers [97, 71]. When an electric field (on the order of megavolts) is applied, the isotropically oriented liquid crystal molecules (*mesogens*) are aligned along the field lines, resulting in an overall deformation [71, 48]. A strain output of ~ 30% was demonstrated [35]. Beside the need for high voltages, a significant drawback of LCEs is that they can take up to ~ 10^3 s to relax [48, 133, 136]. Electrical artificial muscles can also be activated ionically. These include the ionic polymer-metal composites (IPMCs) [40, 15, 28] and ionic gels [70, 98, 2]. In both cases, the structures with freely moving ions are able to bend when a voltage is applied, resulting in a localized stress due to asymmetrical swelling. Drawbacks of IPMCs include low actuation bandwidth (<100 Hz [28]), high cost of noble metals, issues of drying out and environmental unfriendliness [48].

- Magnetic – Forces can be generated and remotely controlled in a magnet-incorporated compound by applying an external magnetic field. This type of actuators feature high-frequency operations (~ 100 Hz) [36], programmability to generate motion with multiple degrees of freedom with foldable structures [74, 90], and are often ideal for applications such as targeted drug delivery [113, 24, 117] in small-scale confined spaces in environments that can be penetrated through by a magnetic field. The limitations of this type of actuators include lack of scalability and high power consumption [48]. The requirement of external hardware also makes it difficult to integrate them into a fully self-contained system.

- Thermal – A number of soft materials can deform in response to heat either by thermal expansion or phase transition. Two typical examples of phase transitioning based

actuators are shape-memory alloys (SMA) and liquid crystal (LC) materials. The former leverages the shape-memory effects due to the reconfigurable crystal structure of some alloys such as nickel titanium (*nitinol*) [109] while the latter takes advantage of the phase transition between isotropic and anisotropic alignments of mesogens, which can lead to very large strain (>300% [124]) if properly initialized In all cases, however, thermal actuators often suffer from low deactivation speed due to heat dissipation issues and hence a limited bandwidth [105].

- Chemical – Energy released in numerous chemical reactions, such as redox [94, 56], changes in pH [132], and altering of material properties of polymers by a variety of organic solvents and based [72], can lead to the deformation of a number of materials.

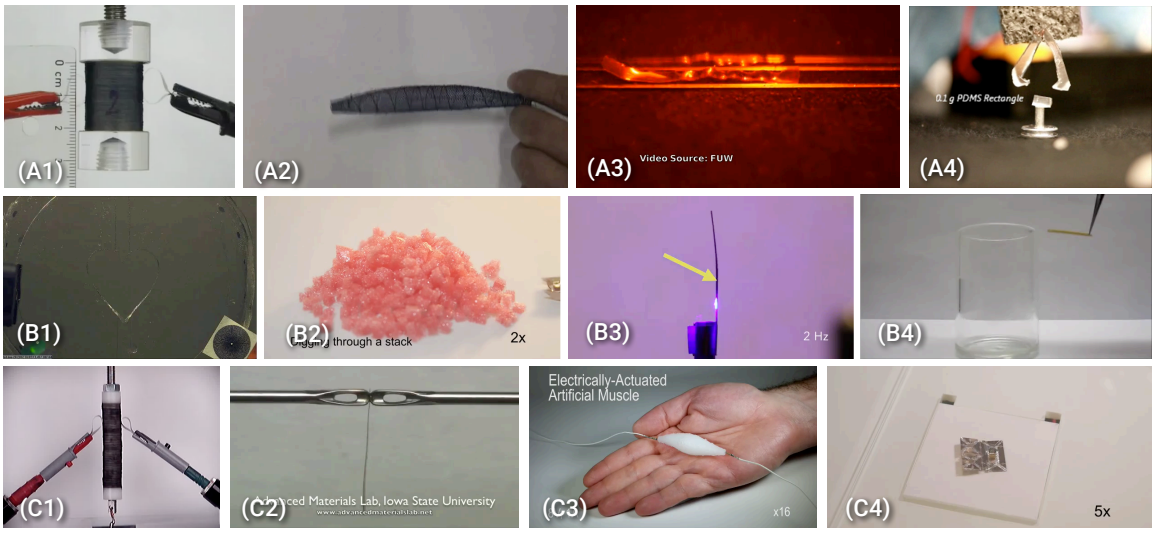

Figure 1.4: Images of previous work on artificial muscles, categorized by materials (A1-A4), energy sources (B1-B4) and actuation principles (C1-C4). (A1) Elastomers (A2) Shape-memory alloys (A3) Liquid crystals (A4) Hydrogels (B1) Electricity (B2) Magnetic Field (B3) Heat (B4) Chemical (C1) Coulomb forces (C2) Ionic diffusion (C3) Phase transition (C4) Magnetic gradients. From [109, 59, 98, 137, 88, 41, 90].

1.2.2 Actuator Performance

The performance of the electrical artificial muscles in Section 1.2.1, including those which are non-ionically driven (DEAs, LCEs) and those which are ionically driven (IPMCs, ionic gels) is summarized in Tables 1.3, 1.4 and 1.5. It is worth noting that the orders of magnitude of operating voltage are correlated to whether an artificial muscle is driven by electric fields (~ kV for DEAs, ~ mV for LCEs) or diffusion of ions (~ V for IPMCs and ionic gels). Another observation is that, while many artificial muscles surpass natural muscles by some metrics (e.g., DEA can output up to ~1,000% compared to ~20% by natural muscles), none matches natural muscles' unique combination of high power-to-mass ratio, wide range of length scales, and long cycle life.

Table 1.3: Properties of selected electrical artificial muscles. Values marked with † are approximate. The (peak) stress represents the maximum force per unit cross-sectional area that an artificial muscle is able to generate. The power-to-mass ratio of IPMCs is calculated by taking the measurement 870 W/m^3 from [7] and the density 1,500 kg/m^3 from [86].

	Strain	Stress	Strain rate	Work density	Power-to-mass
Units	%	MPa	%/s	kJ/m^3	W/kg
Dielectric elastomer (DEA) [48, 87, 57]	10-1,000 †	1-10 †	10^2 †	3,000	0.1
Liquid-crystal elastomer (LCE) [133, 119, 120]	1-30 †	0.25	10^1 †	10 †	
Ionic polymer metallic composites (IPMC) [48, 86, 7, 86]	1-3	3	10^0 †	5.5	0.58
Ionic gels [89]	90	4		460	

Table 1.4: Properties of selected electrical artificial muscles (continued). Values marked with † are approximate. The density and elastic modulus of DEAs are taken as those of VHB 4910 [18] by assuming electrodes with negligible thickness (e.g., 20 nm in [100]). The density and modulus of LCEs are approximated by those of Sylgard 184 (Dow Corning), a common silicone elastomer [55, 30]. Note that the density of liquid crystals in nematic phase is near 1 kg/m^3 [63] and is very similar to that of Sylgard 184. The modulus of IPMCs (>50% hydration) is approximated [95]. The density of ionic gels is approximated by that of water. The modulus of ionic gels is taken as that of typical hydrogels [141].

	Operating voltage	Length scale	Density	Elastic modulus
Units	V	m	kg/m^3	MPa
Dielectric elastomer (DEA) [48, 11, 18]	1–10 kV	1µm–1cm †	960	0.22
Liquid-crystal elastomer (LCE) [48, 39, 133, 71, 30]	1-1,500 kV	1nm-1cm †	982	1 †
Ionic polymer metallic composites (IPMC) [48, 86, 95]	1–5 V †	1µm–1cm †	1,500	100 †
Ionic gels [70, 141]	1–10V	1µm–1cm †	1000	0.1 †

Table 1.5: Properties of selected electrical artificial muscles (continued). The bandwidth represents the range of frequencies at which an artificial muscle can be continuously activated.

	Efficiency	Bandwidth	Cycle life
Units	%	Hz	cycles
Dielectric elastomer (DEA) [89, 59]	90	10 k	10^6
Liquid-crystal elastomer (LCE) [129, 71]	75	133	
Ionic polymer metallic composites(IPMC) [48, 86]	1.5	100	
Ionic gels [112]		0.5	

To better compare the performance between natural and artificial muscles, Figures 1.5, 1.6 and 1.7 show the plots of some selected properties.

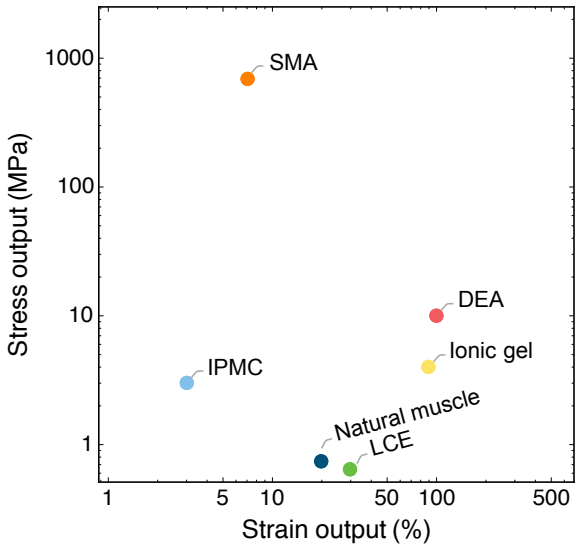

Figure 1.5: Plot of stress vs. strain output of natural muscles, electric motor, and electrical artificial muscles. Note that some values are cited from different sources and approximate as in Table 1.3. Plot scales are logarithmic.

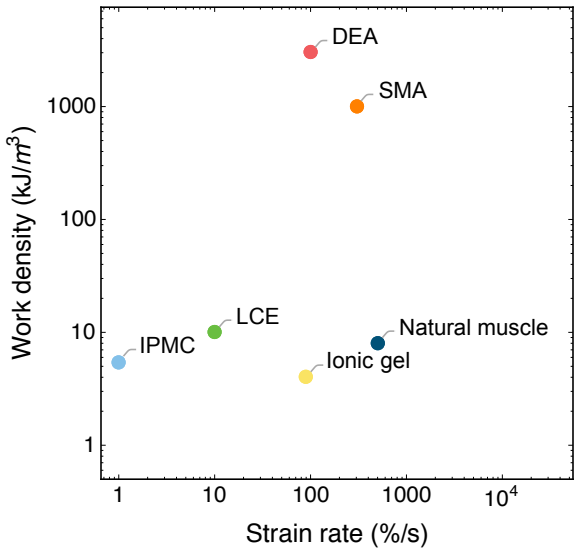

Figure 1.6: Plot of work density vs. strain rate of natural muscles, electric motor, and electrical artificial muscles. Note that some values are cited from different sources and approximate as in Table 1.3. Plot scales are logarithmic.

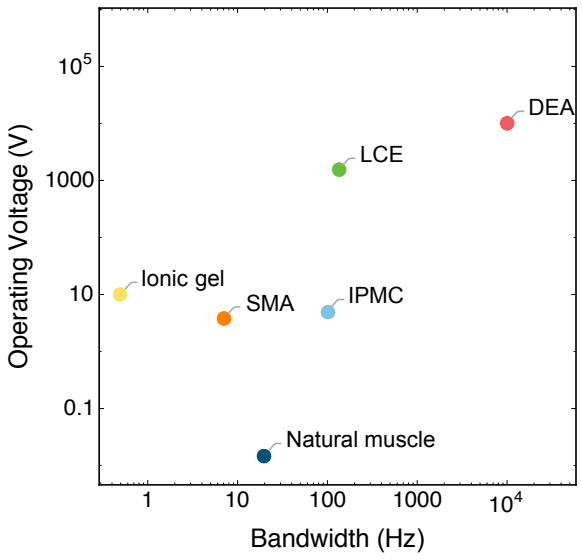

Figure 1.7: Plot of operating voltage vs. bandwidth (highest operating frequency) of natural muscles, electric motor, and electrical artificial muscles. Note that some values are cited from different sources and approximate as in Tables 1.4 and 1.5. Plot scales are logarithmic.

1.3 Overview of Surface Tension Based Actuation

Surface tension is a highly promising principle for building actuators at miniature scales, where the stress output ($\sigma = F \cdot L^{-2}$) given by surface tension (which has units of N/m) scales with dimension by $\sigma \propto L^{-1}$. Compared to most other paradigms of actuation (with fixed σ for most actuator whose force output scales with their cross-sectional areas, e.g., natural muscles and DEAs, or with $\sigma \propto L$ because $F \propto L^3$, e.g., magnetic field driven actuators), as the actuator scales down, there will eventually come a size regime in which surface tension becomes dominant [116, 48]. Metals and alloys that are liquid at room temperature are particularly suitable for this type of actuation because of their huge surface tension (normally hundreds of mN/m).

1.3.1 Electrocapillarity

When a liquid metal is in contact with an electrolytic solution, a pair of two parallel arrays of opposite charges, called *electrical double layer*, forms on the surface of the liquid metal [38]. This phenomenon is illustrated in Figure 1.8. Since all metals are good electrical conductors (e.g., EGaIn has a resistivity of $\sim 29.4 \times 10^{-6}$ ω-cm [23]), the liquid metal of interest here is also referred to as the electrode. Likewise, the electrolyte itself is viewed as the counter-electrode and the reference potential. Interestingly, the surface tension of the liquid metal depends on its potential relative to counter-electrode, a phenomenon called *electrocapillarity* [38]. This can be explained by the fact that the double layer is effectively a capacitor whose charge density changes with electrode potential [25]. Any decrease in the capacitive energy will lead to an increase of the liquid metal and hence changing the surface tension [25].

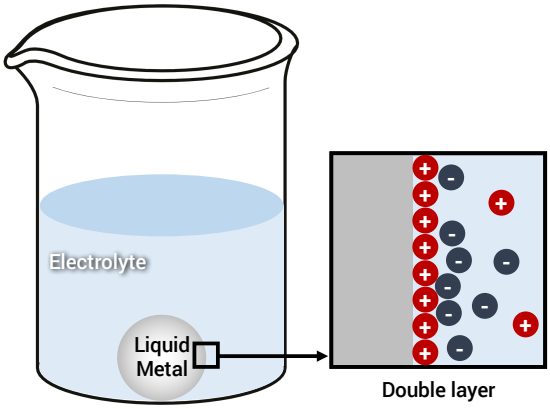

Figure 1.8: Illustration of the formation of an electrical double layer on the metal surface in an electrolyte.

That surface tension can be viewed as a function of potential is ideally captured by the Lippmann equation [38]

$$\frac{d\gamma}{dE} = -q \tag{1.1}$$

where γ is the surface tension of the liquid metal, E is the electrode potential, and q is the charge density on the surface.

Let γ_0 and E_0 be the surface tension and potential at the potential of zero charge (where $q = 0$) respectively. Taking the derivatives of both sides of Equation (1.1) yields

$$\frac{d^2\gamma}{dE^2} = -\frac{dq}{dE} = C_d \tag{1.2}$$

Note that the differential capacitance C_d here is a voltage-independent term [38]. Solving Equations (1.1) and (1.2) for γ gives a clearer form of surface tension-potential relation-

ship [25, 60].

$$\gamma = \gamma_0 + \int_{E_0}^{E} \frac{d\gamma}{dE}\, dE = \gamma_0 - \int_{E_0}^{E} q\, dE = \gamma_0 - \frac{1}{2} C_d \left(E - E_0\right)^2 \tag{1.3}$$

The quadratic function $\gamma(E)$ given by Equation (1.3) is used to characterize liquid metals (e.g., mercury and gallium) in literatures [83, 6, 34]. In summary, electrocapillarity provides a principle of actuation by tuning the surface tension of liquid metals. The operating voltage required to generate some specified force is dependent on the electrocapillary curve of the liquid metal in a certain electrolyte. It should be noted that the surface activity described here, which is characterized by the Lippmann equation, does not involve oxidation on the surface.

1.3.2 Surface Oxidation of Liquid Metal

Apart from electrocapillary tuning of surface tension, liquid metals can also be oxidized on the surface to create an oxide *skin*, which is effectively a surfactant that lowers the surface tension to near zero [60]. This is achieved by immersing the liquid metal into an aqueous solution of hydroxides of alkali metals, such as sodium hydroxide (NaOH) or potassium hydroxide (KOH) [60, 138].

An example is the interaction between an EGaIn droplet and an NaOH solution. At potentials (relative to counter-electrode in NaOH) less oxidative than a certain threshold (~ −1.4 V vs. Ag/AgCl measured by [60]), the surface of EGaIn is oxide-free. Compared to the formation of gallium ions Ga^{3+} in strong acids, in strong basic electrolytes, the $Ga(OH)_4^-$ anions, or *gallate* anions are formed (Figure 1.9). The result is the dissolution of some gal-

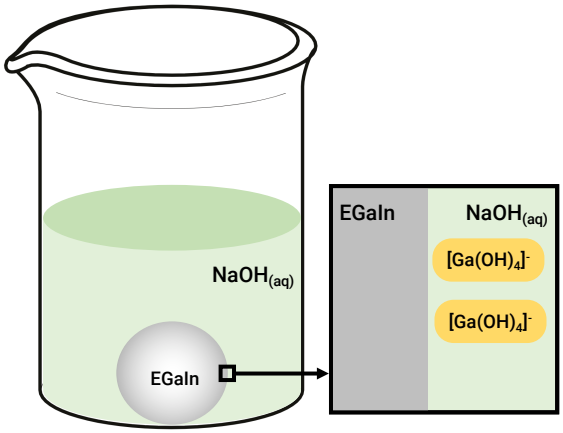

Figure 1.9: Illustration of the dissolution of gallium in a solution of sodium hydroxide (NaOH).

lium on the droplet surface and the forming of sodium gallates $Na\,[Ga(OH)_4]$:

$$2Ga + 2NaOH + 6H_2O \longrightarrow 2Na\,[Ga(OH)_4] + 3H_2 \tag{1.4}$$

At potentials more oxidative than ~ -1.4 V vs. Ag/AgCl [60], an electrolysis of water takes place:

$$2H^+ + 2e^2 \longrightarrow H_2 \qquad \text{(reduction at cathode)} \tag{1.5}$$

$$2H_2O \longrightarrow 4H^+ + O_2 + 4e^- \quad \text{(oxidation at anode)} \tag{1.6}$$

The hydrogen ions created by the oxidation at anode further react with the gallate ions to produce gallium hydroxides $Ga(OH)_3$, which, in turn, produces gallium oxides Ga_2O_3.

$$[Ga(OH)_4]^- + H^+ \longrightarrow Ga(OH)_3 + H_2O \tag{1.7}$$

$$2Ga(OH)_3 \longrightarrow Ga_2O_3 + 3H_2O \tag{1.8}$$

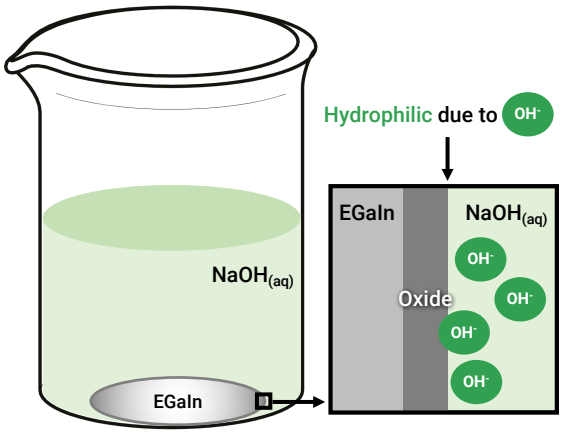

Figure 1.10: Illustration of gallium oxide skin which effectively acts as a surfactant between the EGaIn and NaOH due to the hydrophilicity of Ga_2O_3.

The net result is the formation of a thin coating of Ga_2O_3, or oxide skin, on the surface of EGaIn. This process [1] (shown in Figure 1.10) is completely reversible by reductive capillarity (called *recapillarity* [60]), with little hysteresis, wherein Ga_2O_3 can be removed by lowering the electrode potential [60] to expose the reduced EGaIn.

Compared to reduced EGaIn, where the Gibbs free energy is high in the interface between EGaIn and NaOH, the EGaIn enclosed by oxide skin has effectively two interfaces – i.e., a Ga-Ga_2O_3 interface (which consists of Ga atoms [104]) and a Ga_2O_3-$NaOH_{aq}$ interface (which is hydrophilic due to the OH^- on the surface of Ga_2O_3). This hydrophilicity is illustrated in Figure 1.10.

Overall, the oxide skin acts like a surfactant, which lowers the interfacial tension to near zero [60], providing an opportunity to electrochemically manipulate the surface tension with smaller voltages. In contrast to the oxide-free regime, where the surface tension grows parabolically, with the presence of oxide skin the surface tension drops exponentially ($\gamma \propto \exp(-E/E_0)$ [125]). Figure 1.11 shows this remarkable phenomenon, where, as the

[1] The reactions are verified by Yun-Sik Ohm.

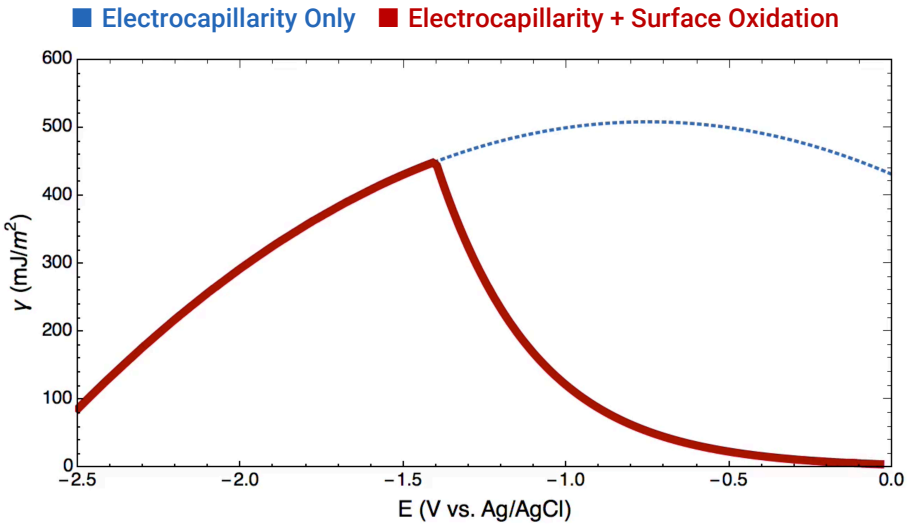

Figure 1.11: Comparison of the interfacial tension-potential relationship using electrocapillarity only and using electrocapillarity with surface oxidation. Data reproduced from [60].

electrode potential increases, the surface tension of liquid metal drops dramatically by oxidation than by electrocapillarity alone.

As seen in Equations (1.4) and (1.6), a continuous formation of hydrogen gas is inevitable. [138] viewed this eruption of gas bubbles as a result of a combination of galvanic interaction and a band structure of gallium. [60] and [106] also reported this phenomenon.

1.4 Thesis Objectives

This work builds upon the principles of surface tension control of liquid metals and seeks to formulate a paradigm for building soft-matter artificial muscles with a unique combination of properties and performance.

Specific goals are summarized as follows:

- *Demonstration of a Scalable Contractile Structure* – To design an elastic hybrid structure composed of a helical spring and liquid metal that is able to perform mechanical work by electrochemically controlling the surface tension of liquid metal immersed in an aqueous solution of sodium hydroxide. The actuators will be experimentally characterized to examine the relationship between electrical potential and actuator length.

- *Proof of Concept for Isolation in Dry Conditions* – To introduce a new form factor of surface tension based actuation by creating a core-shell liquid-hydrogel hybrid wherein the interfacial tension is again controllable by electrochemical deposition and removal of metal oxide. Limitations and issues will be discussed.

A broader perspective is also provided on the role and uniqueness of this artificial muscle paradigm in the current robotics landscape. This thesis concludes with a recommendation for future research on the potential of modularizing the liquid-metal-hydrogel hybrids for repeatable, self-organizing building blocks for robot muscles.

Chapter 2

Helical Spring-Liquid Metal Actuator

Springs are among the most elegant devices to abstract the contractile function of natural muscles (e.g., the Hill-type model [47] represents the mechanical response of a muscle as due to a contractile element plus two spring-like elastic elements. See Figure 2.1). It is therefore intriguing to mimic this behavior by using the controllability of surface tension as the contractile element to *expand* or *compress* the spring for the purpose of constructing an artificial muscle.

Another benefit of incorporating liquid metals into a metallic structure is that most liquid metals wet to most metal substrate very well [27]. With appropriate design and material selection, such a structure can combine the properties of liquid metal (high controllability of surface tension as reviewed in Section 1.3.2) and helical metal spring (Hookean elasticity).

Finally, as an actuator based on surface oxidation described in Section 1.3, only minimal miniaturized electronics is needed to operate. This type of actuator also requires only modest voltages ($\sim$ 1 V), which eliminates the need for bulky power supply units like many other electrically driven artificial muscles.

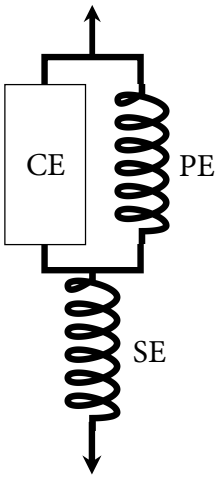

Figure 2.1: Hill-type model for muscle contraction. The nonlinearlity is abstracted by three black boxes: a contractile element (CE) and two spring-like elastic elements in series (SE) and in parallel (PE).

This chapter presents a hybrid structure of artificial muscle (referred to as the *spring-LM actuator*) which is composed of a helical copper spring wetted by EGaIn[1]. Like most other types of artificial muscles, the performance of the spring-LM actuator is benchmarked. Potential applications and limitations of spring-LM actuators are discussed at the end of this chapter.

2.1 Design and Fabrication

The spring-LM actuator proposed here is a device made by wetting EGaIn (75% gallium and 25% indium by weight, ~ $15.5\circ$C melting point [23]) on to the continuous gap between each coil of a helical spring (diameter $D \approx 8.4 \pm 0.2$ mm) handcrafted from a copper wire (diameter $d \approx 0.321$ mm). This design is scalable by altering the number of coils N. In the

[1]In collaboration with Hesham Zaini.

following fabrication and testing $N = 20$. The spring is designed with a hook at the tip for mounting weights. Figure 2.2 is an idealized illustration of this hybrid structure.

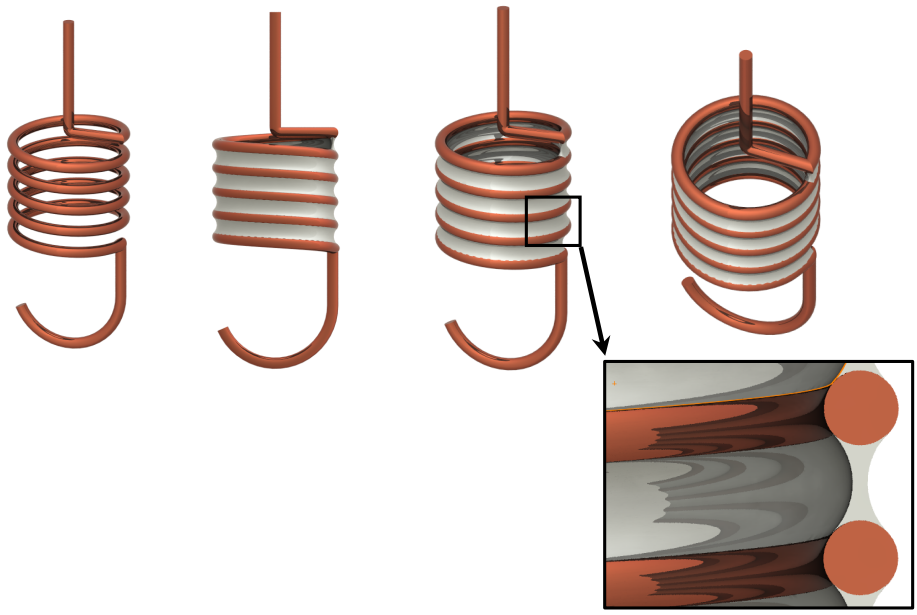

Figure 2.2: Illustration of the design of the spring-LM actuator. Work by Hesham Zaini.

To enhance wettability, the copper oxide on the surface of the spring is removed by immersing the spring in 31.45% w/v hydrochloric acid (HCl) for a few minutes. The spring is then rinsed with isopropanol before carefully wetted with EGaIn.

The spring-LM actuator has to operate in an electrolyte solution, which is necessary for the electrocapillary control of the surface tension. In the following testing a 3% w/v NaOH solution was used. An image of the spring-LM actuator is shown in Figure 2.3.

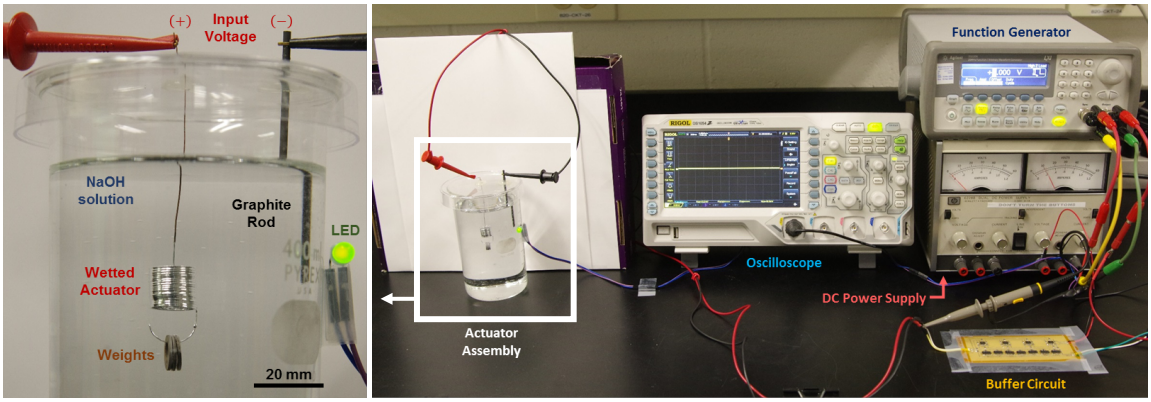

Figure 2.3: Image of the fabrication result and the experimental setup of the spring-LM actuator.

2.2 Experimental Setup

To characterize the relationship between electric potentials and deformation of the spring-LM actuators, experiments were set up as shown in Figure **??**. All potential inputs by the waveform generator (3320A, Agilent's Electronic Measurement Inc.) were with reference to the NaOH solution and buffered by a customized circuit. An oscilloscope (DS1054Z, Rigol Inc.) was used to track the phase of the waveform.

Loads were applied by attaching small washers (≈ 0.226 g) to the lower tip of the spring-LM actuator. In all the loading tests, five different loads were given with zero to four washers.

To measure the axial deformation of the spring-LM actuator, a camera (Pentax K-5 DSLR, Ricoh Inc.) was used to record videos. The lens of the camera was aligned at the center of the actuator to minimize distortion. It should be noted that, although the actuator is submerged in a solution inside a circular-walled beaker and hence the image is distorted by refraction, the difference is ignored. Also, the resolution of this measurement is limited by the camera.

For each loading test, videos were recorded for the actuator lengths in response to two

sets of input waveforms: a triangle wave (period=120 s, symmetric, peaked at -0.5 and +1.0 V) which slowly ramps the potential up and down for quasi-static response and a low-frequency square wave (peaked at -0.5 and +1.0 V) for step response.

2.3 Results and Discussion

Figure 2.4 shows the images of full contraction and expansion of a spring-LM actuator in response to -0.5 V and 1.0 V, respectively. The image analysis is done by tracking the lower tip of the helix. As expected, the spring-LM actuator elongates when the interfacial tension increases due to the deposition of gallium oxide. When this reaction is reversed, the reduction of gallium caused the interfacial tension to increase again, thereby shortens the actuator.

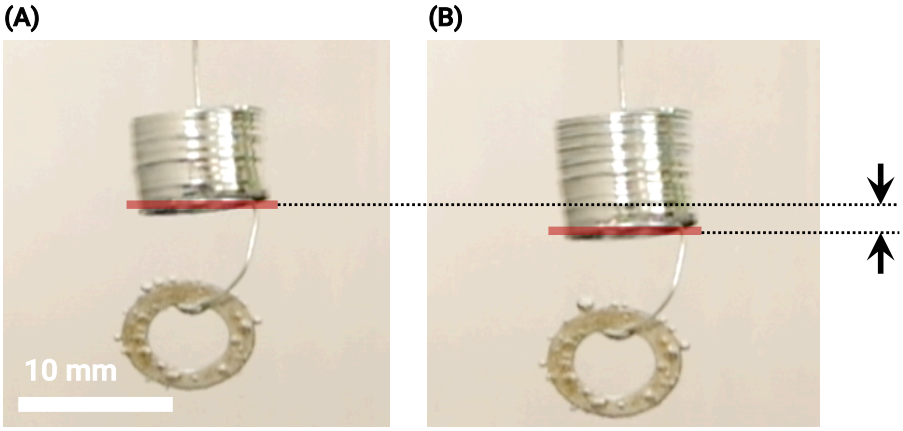

Figure 2.4: Images of (A) full contraction and (B) full expansion of a spring-LM actuator. The full contraction corresponds to -0.5 V and the full expansion corresponds to 1.0 V relative to NaOH solution. The image analysis is done by tracking the lower tip (red line) of the helix. Scale bar represents 10 mm.

2.3.1 Quasi-static Response

To determine the relationship between potential and actuator length, Figure 2.5 shows a plot of data analyzed from the video of testing with zero washers (i.e., no load). When increasing the voltage, a transition happens near 0.8 V which lengthens the actuator by ~1.3 mm. When decreasing the voltage, by contrast, the deformation occurs in two phases, including a modest gradual decrease in length (from 1 V to -0.35 V) followed by a sudden contraction near -0.35 V.

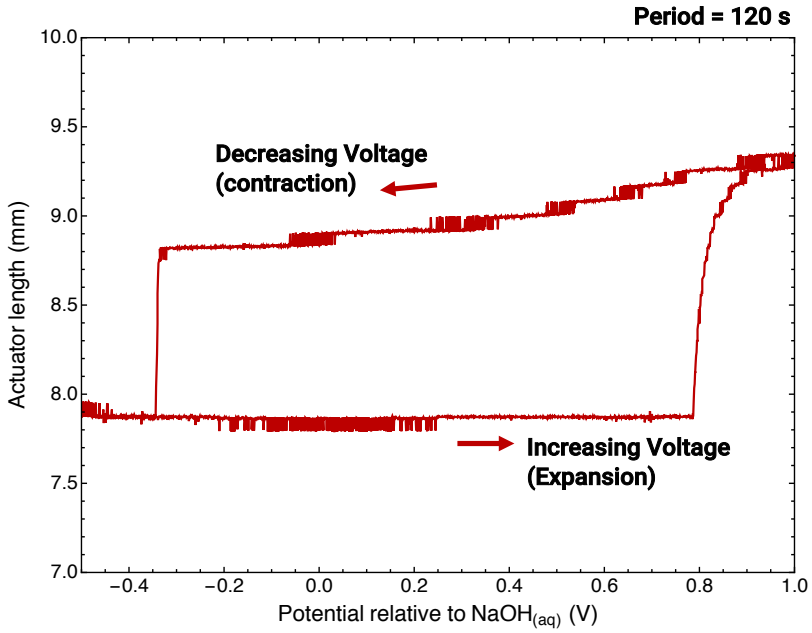

Figure 2.5: Plot of actuator length vs. potential of the electrode relative to NaOH solution with a triangle wave (period: 120 s). The actuator was loaded with zero washers. Data reproduced from the image analysis by Hesham Zaini.

As shown in Figure 2.6 (A), the hysteresis shown in Figure 2.5 is consistent regardless of the number of washers. Also, when varying the load from zero washers ($F = 0$) to four washers ($F = 7.67$ mN), the length change remains almost the same (~ 1.5 mm). It is also

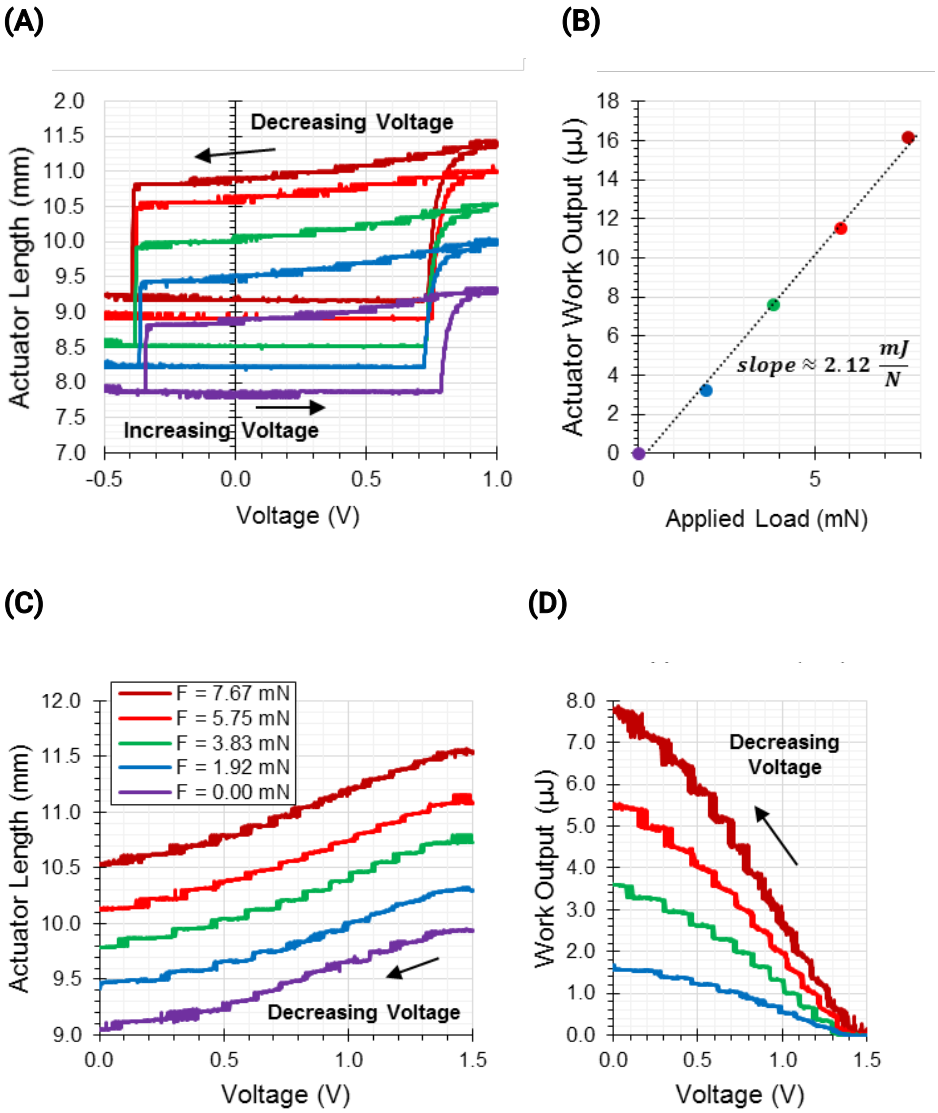

Figure 2.6: Quasi-static analysis of a spring-LM actuator. (A) Plot of actuator length vs. voltage for loads varying from zero washers ($F = 0$) to four washers ($F = 7.67$ mN). (B-D) Work vs. load, length vs. voltage, work vs. voltage taken over the range from 0 to 1.5 V. Data reproduced from the image analysis by Hesham Zaini.

observed that the actuator work output (Figure 2.6 (B)) calculated from the data over the range from 0 to 1.5 V (Figure 2.6 (C)) grows somewhat linearly with the applied load. This is an indication that over this range of gradual decrease in actuator length, the contraction of the actuator does not depend on the applied load but depend on surface reduction and hence restoration of interfacial tension. This is validated by Figure 2.6 (D) where the work output changes linearly with the applied load for any given voltage between 0 and 1.5 V.

2.3.2 Dynamic Response

To characterize the step response of the spring-LM actuator, a low-frequency square wave (peaked at -0.5 and +1.0 V) is applied. The result is shown in Figure 2.7 where the expansion corresponds to a step-up from -0.5 to 1 V and the contraction corresponds to a step-down from 1 to -0.5 V. Once again, the load seems not affecting the behavior of the actuator length. It is observed that expansion occurs smoothly in a similar way to the increasing voltage part of the quasi-static result (Figures 2.5 and 2.5(A)) over the range from 0.8 to 1 V. On the other hand, contraction occurs more rapidly and involves high frequency oscillations that quickly decay with time, as shown in Figure 2.7 (B). It is unclear how factors such as reaction rate and viscosity contribute to this dynamics and the sharp difference between the behaviors of expansion and contraction.

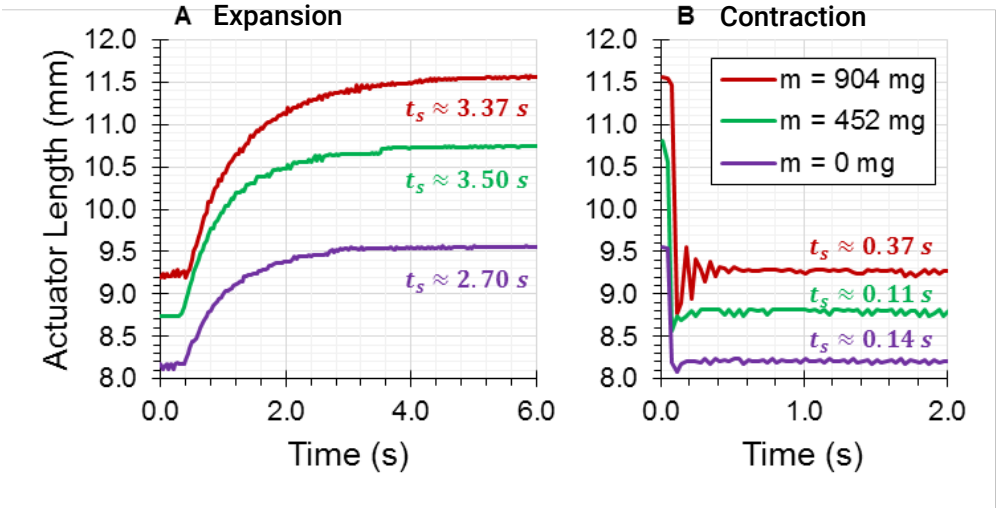

Figure 2.7: Step response of a spring-LM actuator showing (A) step-up from -0.5 to 1 V and (B) step-down from 1 V to -0.5 V. t_s represents the settling time for the actuator tip to enter within 5% of its steady-state position. Data reproduced from the image analysis by Hesham Zaini.

2.3.3 Performance of Spring-Liquid Metal Actuators

From the experiment result, the spring-LM actuators are estimated to have a strain output ~ 18%, a stress output ~ 20.265 kPa, a work density ~ 286.3kJ/m^3 and a strain rate ~ 81%/s. Figures 2.8 and 2.9 show a comparison of spring-LM actuators to natural muscles and selected artificial muscles. It can be seen that the spring-LM actuators have a strain output similar to that of natural muscle and a very high work density.

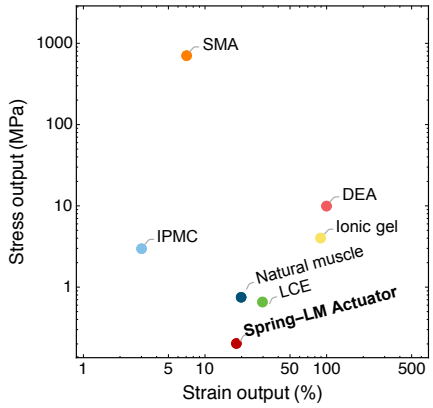

Figure 2.8: Comparison of spring-LM actuators to other actuators in terms of stress output vs. strain output. Values are approximated (Source are the same as Figure 1.5). Stress output is approximated using the cross-sectional area of EGaIn bridges, not the spring.

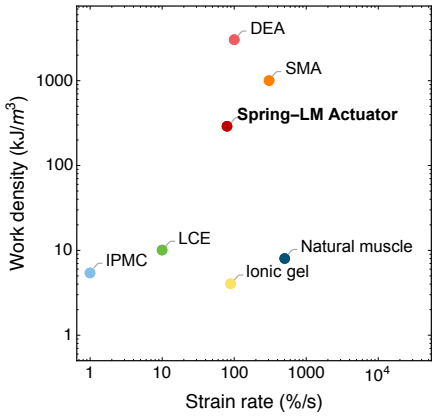

Figure 2.9: Comparison of spring-LM actuators to other actuators in terms of work density vs. strain rate. Values are approximated (Source are the same as Figure 1.6).

2.4 Concluding Remarks

The spring-LM actuators are an elegant realization of muscle-like actuation by elasto-capillarity. Perhaps the most interesting remark is their striking resemblance to some of the features of natural muscles. First, they both take chemical energy, primarily by oxidation, to drive the actuation. Second, they are both *wet* actuators, meaning that they only operate in an aqueous bath of ions. In the case of spring-LM actuators it is the bulk electrolyte solution while for myofibrils it is the sarcoplasm, the cytoplasm of a muscle cell which consists of mostly (75%–80% [76, 110]) water. Also, the combination of passive spring structure and shape-reconfigurable EGaIn distinctively captures the nonlinearity as modeled by Archibald Hill [47].

In theory, surface tension is one of the few physical phenomena which dominates small-scale regimes of actuators because of the scaling law. The helical structure of spring-LM actuator nevertheless can take this advantage into any larger scales by simply making a spring with as many turns as possible at the cost of L rather than L^2.

Their dependence on aqueous environment, however, largely limits their usage unless introducing a new form factor such as gel encapsulation, in which case many other issues can be addressed such as influence of buoyance and dynamics of fluids.

Another downside at present is the eruption of hydrogen gas bubbles from inside the NaOH electrolyte due to an electrolysis of water by galvanic interactions [138]. This is reminiscent of the typical issue of gas build-up in deeply or rapidly charged/discharged lead-acid batteries, for which a number of enhancements have been achieved such as vent valve for gas blow-out and mixing of silica gels to suppress gas formation [99].

There is also plenty of room for improvement of the theoretical model for capillary

bridges between two rod-like solid bodies or even the helical structure itself. Such an improvement will allow for a more accurate model to aid the actuator design in the future. As for the basic understanding of the nonlinearities and time-dependent behaviors as displayed by the spring-LM actuator, more advanced models will need more attention on the dynamics to account for the influence of viscosity and the rheological properties of non-Newtonian regime of gallium oxides.

Chapter 3

Hydrogel-Liquid Metal Hybrids

Muscle cells, or *myocytes*, contain a hydrogel-like cytoplasm (called *sarcoplasm*) where the contraction and self-regulation of all the myofibrils take place in an fluidic environment full of ions. While there has been numerous contending theories of the physical properties of cytoplasm as a whole, many studies identify the *cytosol*, an intracellular fluid as responsible for a number of cellular activities including signaling [61] and metabolite transportation [123]. It is believed that the cytoplasm consists of a polymer matrix formed by a cross-linked cytoskeletal network of long chained molecules (e.g., proteins and polysaccharides, etc.) which altogether displays hydrogel-like features [102, 31]. The solvent contained in the polymer network inside a cell is well-regulated by the cell membrane (or a *sarcolemma* in a myocyte) which separates the fluidic environment from the extracellular space.

From this perspective of cellular biology, an interesting but not yet well-studied approach to synthesize an artificial muscle unit is to create a self-contained artificial *cell* which consists of a membrane-encapsulated liquid that can generate force electrochemically. Clearly, the remarkable controllability of surface tension of liquid metals by electrocapillarity and surface

oxidation is a potential candidate. As discussed in Section 2.5, however, this phenomenon relies on an aqueous electrolyte solution and is not readily usable to build artificial muscles for most dry conditions. To bridge this gap, a hypothetical hydrogel electrolyte which is able to structurally support itself, to carry ions to oxide and reduce the gallium surface, and to elastically resist loads with high stretchability and toughness, will enable a new class of artificial muscles that resemble their biological counterparts.

The use of hydrogels in actuators is not something new. As reviewed in Section 1.2.2, current gel-based actuators are mostly osmotically driven by asymmetric swelling of ions [48, 98, 134, 62]. They are largely limited by slow response time (e.g., minutes to hours [134]) and hence impractical in many robotic applications. Recent advances in the enhancement of mechanical properties, theoretical modeling, and multifunctionalities of hydrogels [115, 135, 49, 73, 13, 139, 14, 82, 134, 75, 50] have shown great promises, many of which are applicable to new schemes of hydrogel-based actuation.

This chapter presents the hydrogel-liquid metal (hydrogel-LM) actuator, a new form factor for surface tension based actuators that combines the properties of liquid metal (elastocapillarity) and hydrogels (low elastic modulus and ability to carry ions). Early demonstration shows evidence that such a form factor is possible to fabricate and promising in future development. Issues and possible solutions are discussed at the end of this chapter.

3.1 Hypothesis

A hypothesis is proposed and examined in this chapter as to the feasibility of the following goals, which are the basis for the proposed hydrogel-LM actuator to function.

- A hybrid of EGaIn and hydrogel (i.e., a caviar-like structure as illustrated in Figure 3.1) can be fabricated in such a way to support its own weight and structure, to isolate the liquid EGaIn from the exterior dry environment, and to prevent leakage.
- Surface oxidation and reduction, as well as electrocapillarity, can take place at the interface between EGaIn and hydrogel electrolyte by ionic diffusion within the gel matrix and result in changes in interfacial tension as in aqueous solution.

It should be noted that the scope of this chapter is limited to the feasibility of the proposed actuation scheme in principle. A practical selection of materials and fabrication steps are presented. Characterization for such an actuator at a specific scale (e.g., ~ μm), in addition to the demonstration for robotic applications, is part of an ongoing work.

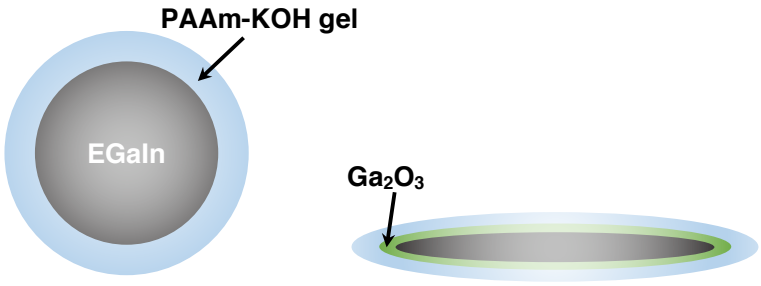

Figure 3.1: Concept of the proposed caviar-like hydrogel-LM structure.

3.2 Design and Fabrication

The design of an hydrogel-LM actuator consists of a small millimeter-scale EGaIn droplet and a hydrogel *membrane* around the liquid EGaIn to provide structural support, ion transport, and prevention of leakage. Figure 3.1 shows the concept of the actuation principle. When the interface between EGaIn and hydrogel is free of gallium oxide, the high interfacial energy causes the EGaIn droplet to try to beads up to minimize the interface area. By electrochemically depositing a gallium oxide skin in between the EGaIn and the hydrogel membrane, the interfacial tension drops significantly and, by the hypothesis, deforms the entire structure. When placed on a flat surface like a Petri dish, a lower surface causes the hydrogel-LM hybrid to flatten due to gravity. Similarly, the hybrid elongates in response to a decrease in surface tension when it is hung vertically. The resultant mechanical work should depend on the size scale of EGaIn droplet, thickness of the hydrogel membrane, gel properties (e.g., modulus, residual stress, pH) and the interfacial bonding of liquid metal and hydrogel surfaces.

3.2.1 Gel Preparation

Polyacrylamide (PAAm) hydrogel that contains potassium hydroxide (KOH) was used as the ionic hydrogel for the following reasons. First, PAAm gels are more easily deformable (Young's modulus ~ 2.307 kPa with 90% water concentration [1]) and less brittle (facture energy ~ 10–50 J/m^2 [96, 10]) than many other hydrogels. Second, It has been shown that PAAm gels can be synthesized with double-crosslinked alginate gels to achieve very high fracture energy (~9000 J/m^2) and high strain (~17) [115] and, therefore, the proposed design here can potentially be made with PAAm-alginate gels in the future for tougher artificial

muscles. Finally, KOH was selected because of its high solubility in water (1,210 g/L at 25°C [45], compared to NaOH's 1,110 g/L) and hence higher ionic conductivity per unit volume.

The ionic hydrogel was synthesized by first dissolving powders of acrylamide monomers (AAM, Sigma-Aldrich, A8887) into deionized water by 40 wt%. The AAm solution was then mixed into a 50 wt% KOH solution (Factory Direct Chemicals, Inc., 0.88 of the weight of AAm solution) and then diluted by adding more deionized water (2.5984 the weight of AAm solution). *N,N*-methylenebisacrylamide (MBAA, Sigma-Aldrich, M7279, 0.002 the weight of AAm solution) was added as the crosslinker and ammonium persulfate (AP, Sigma-Aldrich, A8887, 0.006 the weight of AAm solution) was added as a photoinitiator to provide free radicals under ultraviolet light (UV). Right before curing, *N,N,N',N'*-tetramethylethylenediamine (TEMED, Sigma-Aldrich, T7024, 0.0048 the weight of AAm solution) was added to the pre-gel solution as a crosslinking accelerator. A UV nail lamp (MelodySusie, 54W, 365 nm) was used to cure the hydrogels.

3.2.2 EGaIn Deposition

The EGaIn, depending on fabrication techniques, can be deposited before or after the hydrogel is cured. The following demonstration is done by using a pipette to place a EGaIn droplet on the surface of a sample of cured PAAm-KOH hydrogel. Due to the high density of EGaIn (6.095 g/mL [130]) and self-healing property of hydrogels, the EGaIn droplet quickly sinks to the bottom and becomes surrounded by the hydrogel.

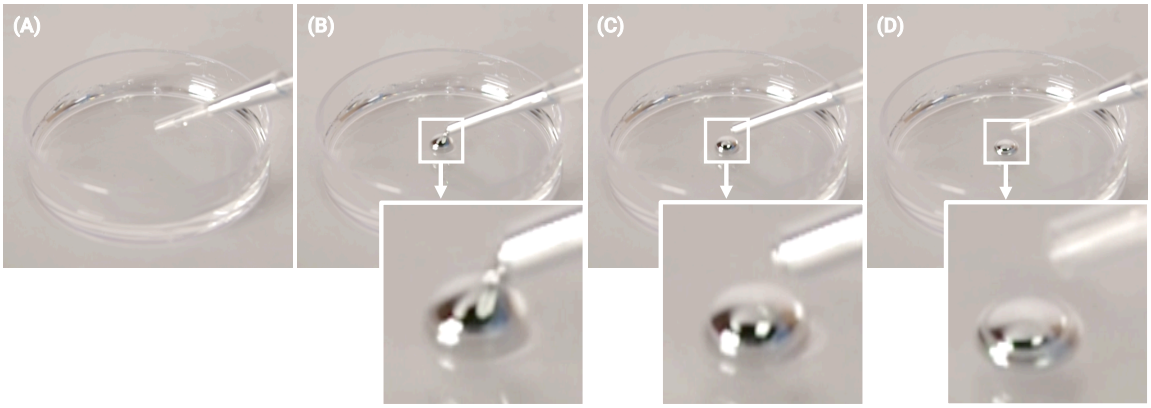

Figure 3.2: An EGaIn droplet being deposited into a sample of cured PAAm-KOH hydrogel.

3.3 Result and Discussion

Simplistic tests similar to that described in Section 2.2 were carried out for successful sample of hydrogel-LM hybrids. The electrode for the EGaIn was done by piercing the hydrogel wall with a copper wire that eventually went in contact with EGaIn. Another copper wire was adhered to the exterior of the hydrogel as a counter electrode. A square wave (1 Hz, ±2 V) was applied. This setup is shown in Figure 3.3.

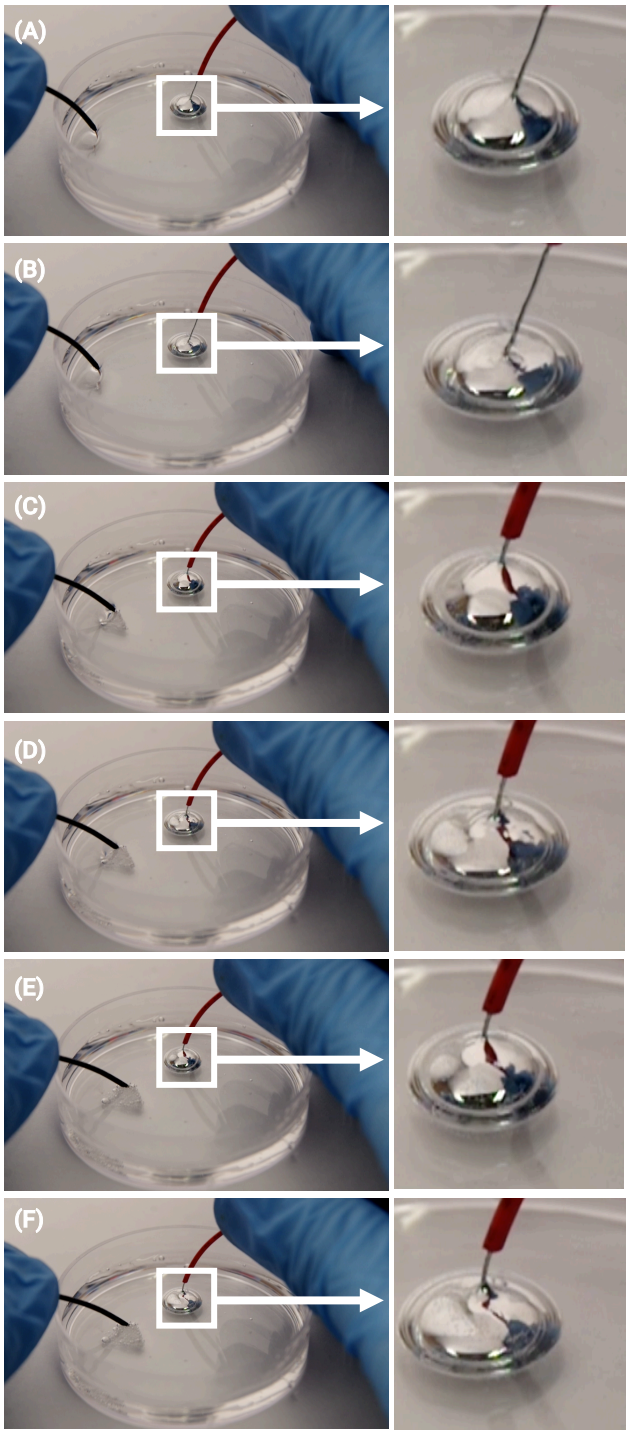

Figure 3.3: Demonstration of EGaIn heartbeats inside the PAAm-KOH hydrogel. Hydrogen gas bubbles can be seen at the electrodes.

As a result, the EGaIn droplet shows visible heartbeat-like motion inside the PAAm-KOH hydrogel in response to the 1 Hz square wave. Despite being surrounded by gels, the shape of the EGaIn droplet flattens due to gravity when the interfacial tension decreases with the presence of gallium oxide. When the gallium is reduced, the EGaIn droplet restores its original shape by beading up in an attempt to minimize the interfacial area. This indicates that it is possible to for electrocapillarity and surface oxidation/reduction to take place at the interface between liquid metal and hydrogel electrolyte by ionic diffusion. It is also observed that hydrogen gas bubbles are formed at the electrodes, which is another indication that supports the hypothesis that a redox reaction is happening in the hydrogel. All these are supporting evidence that hydrogels are a promising medium for the shape reconfiguration of liquid metal.

3.4 Concluding Remarks

The practicality of the hydrogel-LM actuator is highly dependent on the size scale by the scaling law. Intuitively, the effect of surface tension that allows EGaIn droplet to deforms the gel membrane is more dominant at millimeter or even micrometer scales (compared to the length of a sarcomere ~ 2 μm [101, 21]). The proof of concept, however, is hindered by the lack of a scalable fabrication scheme to synthesize a hydrogel-LM hybrid in which the small-scale LM droplet bonds to the surrounding hydrogels membrane, which is thick and tough enough to prevent rupture and thin enough to allow stretchability. A theoretical formulation of hydrogel-LM interaction is also needed to aid the parameter selection in order to maximize the output strain and work density.

Like the spring-LM actuator, gas formation remains a significant issue. Apart from

searching for new chemical reactions to lower the surface tension, an interesting direction for future research is to mimic the vesicle transport and selective filtering mechanisms in cells [9]. Unlike the spring-LM actuator, whose copper wire itself serves as the electrode for voltage input, the hydrogel-LM actuator needs to be integrated with other electronics, preferably using stretchable conducting materials. This will have an effect on the design and modeling. Biological insights from neuromuscular junctions can be beneficial.

The key role in the interaction between EGaIn and hydrogel is how well the gel matrix bonds to liquid metals surface at a molecular level. Since the bond transmits the deformation of EGaIn to that of gel and vice versa, it contributes to the overall actuator response. A theoretical formulation will provide more insights to the physics of hydrogel-LM actuator.

For robotic applications, like all other types of artificial muscles, the hydrogel-LM actuator will require a means of integration into a robot. Natural muscles answer this question by growing around the muscle an outer envelope, or *epimysium*, which anchors the muscle to a tendon that, in turn, connect to a bone. An artificial equivalent to these connective tissue will be one of the steps that are essential to scale up from artificial muscles to tissue, to muscular system, and finally, to a like-like robot.

Chapter 4

Conclusion and Future Research

It is demonstrated in this work that surface tension is a highly promising and practical principle for building artificial muscles. Liquid metals, in particular, are identified as a soft matter that shows remarkable controllability of surface tension by electrocapillarity and surface oxidation. Hybrids that combine liquid metals with other soft matters such as gels further display resemblance to muscles in Nature.

The objectives proposed in Section 1.4 are achieved by presenting two different form factors of surface tension based artificial muscles. A scalable contractile hybrid structure (i.e., the spring-LM actuator) that is capable of lifting loads by electrochemically controlling the surface tension of liquid metals is demonstrated in Chapter 2. The same principles further evolve into another form factor (i.e., the hydrogel-LM actuator), which combines the elasto-capillarity of liquid metals and stretchability, toughness and ionic conductivity of hydrogels, is presented in Chapter 3. It is shown that this caviar-like hybrid, despite some limitations, is feasible to fabricate and capable of generate force and motion in response to an electrical impulse. Both actuators are an elegant device that abstracts some aspects of

natural muscles.

Recent advances in artificial muscles have transformed the robotics landscape. Nevertheless, they are mostly developed, to varying degrees, from a high-level and top-down approach in which the complexity of biological muscular system is often unnecessarily abstracted. Typical examples are McKibben pneumatic actuators and dielectric elastomers; the former are essentially balloons and the latter rubber stacks, both of which cannot capture most aspects of the muscle hierarchy (Figure 1.3). It is argued here that the quest for more muscle-like actuators should better be approached bottom-up, where basic motor units, or *cells*, can be hierarchically assembled into *tissue*, *organ*, *system* and ultimately a *being*. This is analogous to the renaissance of artificial intelligence in the last decade where a powerful neural network is built upon simple neurons that abstract[1] a lowest level of biological neural system.

As stated in Section 3.4, surface tension based actuation is theoretically much more powerful at very small (~ μm) scale. This is comparable to a *sarcomere*, a basic contractile unit in natural muscles which has a length ~ 2μm and a typical force output ~ 2 pF [101, 21]. In this regard, building artificial muscles from basic μm-scale units has the potential to achieve the overall resemblance to biological muscles at higher levels. The paradigm presented in this work is shown to be a promising way to construct such a unit.

In addition to conventional benchmarks for artificial muscles by comparison to muscles in Nature, it is noteworthy that many qualitative characteristics of biological muscles, which have not yet received much attention in artificial muscles community, are also significant for an animal to function. As mentioned in Section 1.1, the ability to store energy

[1] What is life? John von Neumann answered this question by "Life is a process which can be *abstracted* away from any particular medium."

and power themselves and the self-healing, growth and long-term adaptability, are among the most interesting aspects of biological muscles that are not widely mimicked in robotic systems. Recent advances in soft materials such as hydrogel-based power source [107] and self-healing composite of liquid metal and elastomer [85] suggest an interesting direction for future research on soft-matter artificial muscles.

Bibliography

[1] Yara Abidine et al. "Physical properties of polyacrylamide gels probed by AFM and rheology". In: *EPL (Europhysics Letters)* 109.3 (2015), p. 38003.

[2] Suk-kyun Ahn et al. "Stimuli-responsive polymer gels". In: *Soft Matter* 4.6 (2008), pp. 1151–1157.

[3] Samin Akbari. "Arrays of dielectric elastomer microactuators for cell mechanotransduction". PhD thesis. EPFL, 2013.

[4] Haruhiko Asada and Takeo Kanade. "Design of direct-drive mechanical arms". In: *Journal of Vibration, Acoustics, Stress, and Reliability in Design* 105.3 (1983), pp. 312–316.

[5] Haruhiko Asada, Takeo Kanade, and Ichiro Takeyama. "Control of a direct-drive arm". In: *Journal of Dynamic Systems, Measurement, and Control* 105.3 (1983), pp. 136–142.

[6] IA Bagotskaya, AM Morozov, and NB Grigoryev. "On the zero-charge potential of gallium in aqueous solutions and the origin of high capacitance at the gallium/solution interface". In: *Electrochimica Acta* 13.4 (1968), pp. 873–879.

[7] Xiaoqi Bao, Yoseph Bar-Cohen, and Shyh-Shiuh Lih. "Measurements and macro models of ionomeric polymer-metal composites (IPMC)". In: *Smart Structures and Materials 2002: Electroactive Polymer Actuators and Devices (EAPAD)*. Vol. 4695. International Society for Optics and Photonics. 2002, pp. 220–228.

[8] John Jairo Hoyos Betancur. *Generalidades Del System Muscular*. 2014. URL: https://www.slideshare.net/grupoodonto20132/muscular-generalidades-del-sistema (visited on 08/13/2018).

[9] Nicole Billings et al. "Material properties of biofilms—a review of methods for understanding permeability and mechanics". In: *Reports on Progress in Physics* 78.3 (2015), p. 036601.

[10] Daniel Bonn et al. "Delayed fracture of an inhomogeneous soft solid". In: *Science* 280.5361 (1998), pp. 265–267.

[11] Michael Bozlar et al. "Dielectric elastomer actuators with elastomeric electrodes". In: *Applied Physics Letters* 101.9 (2012), p. 091907.

[12] Trevor A Branch et al. "Past and present distribution, densities and movements of blue whales Balaenoptera musculus in the Southern Hemisphere and northern Indian Ocean". In: *Mammal Review* 37.2 (2007), pp. 116–175.

[13] Damien Calvet, Joyce Y Wong, and Suzanne Giasson. "Rheological monitoring of polyacrylamide gelation: Importance of cross-link density and temperature". In: *Macromolecules* 37.20 (2004), pp. 7762–7771.

[14] Hon Fai Chan et al. "Folding artificial mucosa with cell-laden hydrogels guided by mechanics models". In: *Proceedings of the National Academy of Sciences* (2018), p. 201802361.

[15] Zheng Chen, Tae I Um, and Hilary Bart-Smith. "Ionic polymer-metal composite enabled robotic manta ray". In: *Electroactive Polymer Actuators and Devices (EAPAD) 2011*. Vol. 7976. International Society for Optics and Photonics. 2011, p. 797637.

[16] Nick Cheney and Hod Lipson. "Topological evolution for embodied cellular automata". In: *Theoretical Computer Science* 633 (2016), pp. 19–27.

[17] Nick Cheney et al. "Unshackling evolution: evolving soft robots with multiple materials and a powerful generative encoding". In: *Proceedings of the 15th annual conference on Genetic and evolutionary computation*. ACM. 2013, pp. 167–174.

[18] The 3M Company. *VHB Tape Specialty Tapes: Technical Data*. `https://multimedia.3m.com/mws/media/9866950/3m-vhb-tape-specialty-tapes.pdf`. Accessed: 2018-07-29. 2015.

[19] Roger Cooke. "The sliding filament model: 1972–2004". In: *The Journal of general physiology* 123.6 (2004), pp. 643–656.

[20] GM Cooper. *Structure and organization of actin filaments*. Sinauer Associates, 2000.

[21] Alison Cutts. "The range of sarcomere lengths in the muscles of the human lower limb." In: *Journal of anatomy* 160 (1988), p. 79.

[22] Amir Degani et al. "Highly articulated robotic probe for minimally invasive surgery". In: *Robotics and Automation, 2006. ICRA 2006. Proceedings 2006 IEEE International Conference on*. IEEE. 2006, pp. 4167–4172.

[23] Michael D Dickey et al. "Eutectic gallium-indium (EGaIn): a liquid metal alloy for the formation of stable structures in microchannels at room temperature". In: *Advanced Functional Materials* 18.7 (2008), pp. 1097–1104.

[24] Eric Diller et al. “Six-degree-of-freedom magnetic actuation for wireless microrobotics”. In: *The International Journal of Robotics Research* 35.1-3 (2016), pp. 114–128.

[25] Collin B Eaker and Michael D Dickey. “Liquid metal actuation by electrical control of interfacial tension”. In: *Applied Physics Reviews* 3.3 (2016), p. 031103.

[26] Sarah F Eby et al. “Shear wave elastography of passive skeletal muscle stiffness: influences of sex and age throughout adulthood”. In: *Clinical biomechanics* 30.1 (2015), pp. 22–27.

[27] Nicolas Eustathopoulos. “Wetting by liquid metals—application in materials processing: the contribution of the Grenoble group”. In: *Metals* 5.1 (2015), pp. 350–370.

[28] Bo-Kai Fang, Chou-Ching K Lin, and Ming-Shaung Ju. “Development of sensing/actuating ionic polymer–metal composite (IPMC) for active guide-wire system”. In: *Sensors and Actuators A: Physical* 158.1 (2010), pp. 1–9.

[29] Adam W Feinberg et al. “Muscular thin films for building actuators and powering devices”. In: *Science* 317.5843 (2007), pp. 1366–1370.

[30] Angel S Cruz Félix et al. “Physical-chemical properties of PDMS samples used in tunable lenses”. In: *Int. J. Eng. Sci. Innovative Technol* 3.2 (2014), pp. 563–571.

[31] Johannes Fels, Sergei N Orlov, and Ryszard Grygorczyk. “The hydrogel nature of mammalian cytoplasm contributes to osmosensing and extracellular pH sensing”. In: *Biophysical journal* 96.10 (2009), pp. 4276–4285.

[32] Jeffrey T Finer, Robert M Simmons, and James A Spudich. “Single myosin molecule mechanics: piconewton forces and nanometre steps”. In: *Nature* 368.6467 (1994), p. 113.

[33] T Førland. "On the mechanism of muscular contraction." In: *Biophysical journal* 47.5 (1985), p. 665.

[34] A Frumkin et al. "Electrocapillary phenomena on gallium". In: *Electrochimica Acta* 10.8 (1965), pp. 793–802.

[35] Yuuta Fuchigami, Toshikazu Takigawa, and Kenji Urayama. "Electrical actuation of cholesteric liquid crystal gels". In: *ACS Macro Letters* 3.8 (2014), pp. 813–818.

[36] Piotr Garstecki et al. "Propulsion of flexible polymer structures in a rotating magnetic field". In: *Journal of Physics: Condensed Matter* 21.20 (2009), p. 204110.

[37] Richard H Gaylord. *Fluid actuated motor system and stroking device*. US Patent 2,844,126. 1958.

[38] David C Grahame. "The electrical double layer and the theory of electrocapillarity." In: *Chemical reviews* 41.3 (1947), pp. 441–501.

[39] Tyler Guin et al. "Electrical Control of Shape in Voxelated Liquid Crystalline Polymer Nanocomposites". In: *ACS applied materials & interfaces* 10.1 (2017), pp. 1187–1194.

[40] Shuxiang Guo, Toshio Fukuda, and Kinji Asaka. "A new type of fish-like underwater microrobot". In: *Ieee/Asme Transactions on Mechatronics* 8.1 (2003), pp. 136–141.

[41] Carter S Haines et al. "Artificial muscles from fishing line and sewing thread". In: *science* 343.6173 (2014), pp. 868–872.

[42] John E. Hall. "Guyton and Hall Textbook of Medical Physiology, 13th Edition". In: Saunders, 2015, p. 183. ISBN: 1455770051.

[43] Wendie Hamelink et al. *Muscle Contraction on the Molecular Level: Actin-myosin Interaction Studied in an in Vitro Motility Assay*. Universiteit van Amsterdam [Host], 1999.

[44] A John Harris et al. "Muscle fiber and motor unit behavior in the longest human skeletal muscle". In: *Journal of Neuroscience* 25.37 (2005), pp. 8528–8533.

[45] William M Haynes. *CRC handbook of chemistry and physics*. CRC press, 2014.

[46] Zhen-He He et al. "ATP consumption and efficiency of human single muscle fibers with different myosin isoform composition". In: *Biophysical journal* 79.2 (2000), pp. 945–961.

[47] Archibald Vivian Hill. "The heat of shortening and the dynamic constants of muscle". In: *Proc. R. Soc. Lond. B* 126.843 (1938), pp. 136–195.

[48] Lindsey Hines et al. "Soft Actuators for Small-Scale Robotics". In: *Advanced Materials* 29.13 (2017), p. 1603483.

[49] Sungmin Hong et al. "3D printing of highly stretchable and tough hydrogels into complex, cellularized structures". In: *Advanced materials* 27.27 (2015), pp. 4035–4040.

[50] Wei Hong, Xuanhe Zhao, and Zhigang Suo. "Large deformation and electrochemistry of polyelectrolyte gels". In: *Journal of the Mechanics and Physics of Solids* 58.4 (2010), pp. 558–577.

[51] Chris Hughes. *Skeletal Muscle Structure, Function, and Plasticity: The Physiological Basis of Rehabilitation*. Vol. 35. 4. Medicine & Science in Sports & Exercise, 2003, p. 710.

[52] Ian W Hunter and Serge Lafontaine. "A comparison of muscle with artificial actuators". In: *Solid-State Sensor and Actuator Workshop, 1992. 5th Technical Digest., IEEE*. IEEE. 1992, pp. 178–185.

[53] Andrew F Huxley and R Niedergerke. "Structural changes in muscle during contraction: interference microscopy of living muscle fibres". In: *Nature* 173.4412 (1954), p. 971.

[54] Akihiko Ishijima et al. "Sub-piconewton force fluctuations of actomyosin in vitro". In: *Nature* 352.6333 (1991), p. 301.

[55] ID Johnston et al. "Mechanical characterization of bulk Sylgard 184 for microfluidics and microengineering". In: *Journal of Micromechanics and Microengineering* 24.3 (2014), p. 035017.

[56] Bala Krishna Juluri et al. "A mechanical actuator driven electrochemically by artificial molecular muscles". In: *Acs Nano* 3.2 (2009), pp. 291–300.

[57] Nicholas Kellaris et al. "Peano-HASEL actuators: Muscle-mimetic, electrohydraulic transducers that linearly contract on activation". In: *Science Robotics* 3.14 (2018), eaar3276.

[58] Christoph Keplinger et al. "Harnessing snap-through instability in soft dielectrics to achieve giant voltage-triggered deformation". In: *Soft Matter* 8.2 (2012), pp. 285–288.

[59] Christoph Keplinger et al. "Stretchable, transparent, ionic conductors". In: *Science* 341.6149 (2013), pp. 984–987.

[60] Mohammad Rashed Khan et al. “Giant and switchable surface activity of liquid metal via surface oxidation”. In: *Proceedings of the National Academy of Sciences* 111.39 (2014), pp. 14047–14051.

[61] Boris N Kholodenko. “Four-dimensional organization of protein kinase signaling cascades: the roles of diffusion, endocytosis and molecular motors”. In: *Journal of Experimental Biology* 206.12 (2003), pp. 2073–2082.

[62] Youn Soo Kim et al. “Thermoresponsive actuation enabled by permittivity switching in an electrostatically anisotropic hydrogel”. In: *Nature materials* 14.10 (2015), p. 1002.

[63] Young-Ki Kim, Bohdan Senyuk, and Oleg D Lavrentovich. “Molecular reorientation of a nematic liquid crystal by thermal expansion”. In: *Nature communications* 3 (2012), p. 1133.

[64] Kazuo Kitamura et al. “A single myosin head moves along an actin filament with regular steps of 5.3 nanometres”. In: *Nature* 397.6715 (1999), p. 129.

[65] Glenn K Klute, Joseph M Czerniecki, and Blake Hannaford. “Artificial muscles: Actuators for biorobotic systems”. In: *The International Journal of Robotics Research* 21.4 (2002), pp. 295–309.

[66] Glenn K Klute, Joseph M Czerniecki, and Blake Hannaford. “McKibben artificial muscles: pneumatic actuators with biomechanical intelligence”. In: *Advanced Intelligent Mechatronics, 1999. Proceedings. 1999 IEEE/ASME International Conference on*. IEEE. 1999, pp. 221–226.

[67] R Kornbluh, R Pelrine, and J Joseph. “Electrostriction of polymer dielectrics with compliant electrodes as a means of actuation”. In: *Sens. Actuat* 64 (1998), pp. 77–85.

[68] Alex Krizhevsky, Ilya Sutskever, and Geoffrey E Hinton. "Imagenet classification with deep convolutional neural networks". In: *Advances in neural information processing systems*. 2012, pp. 1097–1105.

[69] Ivana Y Kuo and Barbara E Ehrlich. "Signaling in muscle contraction". In: *Cold Spring Harbor perspectives in biology* 7.2 (2015), a006023.

[70] Gu Han Kwon et al. "Biomimetic soft multifunctional miniature aquabots". In: *Small* 4.12 (2008), pp. 2148–2153.

[71] W Lehmann et al. "Giant lateral electrostriction in ferroelectric liquid-crystalline elastomers". In: *Nature* 410.6827 (2001), p. 447.

[72] Timothy G Leong et al. "Tetherless thermobiochemically actuated microgrippers". In: *Proceedings of the National Academy of Sciences* (2009), pnas–0807698106.

[73] Jianyu Li et al. "Hybrid hydrogels with extremely high stiffness and toughness". In: *ACS Macro Letters* 3.6 (2014), pp. 520–523.

[74] Shuguang Li et al. "Fluid-driven origami-inspired artificial muscles". In: *Proceedings of the National Academy of Sciences* (2017), p. 201713450.

[75] Shaoting Lin et al. "Stretchable hydrogel electronics and devices". In: *Advanced Materials* 28.22 (2016), pp. 4497–4505.

[76] Anne Listrat et al. "How muscle structure and composition influence meat and flesh quality". In: *The Scientific World Journal* 2016 (2016).

[77] Alexander G Liu et al. "Haootia quadriformis n. gen., n. sp., interpreted as a muscular cnidarian impression from the Late Ediacaran period (approx. 560 Ma)". In: *Proc. R. Soc. B* 281.1793 (2014), p. 20141202.

[78] John D Madden. "Mobile robots: motor challenges and materials solutions". In: *science* 318.5853 (2007), pp. 1094–1097.

[79] John DW Madden et al. "Artificial muscle technology: physical principles and naval prospects". In: *IEEE Journal of oceanic engineering* 29.3 (2004), pp. 706–728.

[80] Carmel Majidi. "Soft robotics: a perspective—current trends and prospects for the future". In: *Soft Robotics* 1.1 (2014), pp. 5–11.

[81] Richa Malhotra. *Watch this caterpillar fling its beetle attacker through the air*. 2018. URL: http://www.sciencemag.org/news/2018/02/watch-caterpillar-fling-its-beetle-attacker-through-air (visited on 08/03/2018).

[82] Yunwei Mao et al. "A large deformation viscoelastic model for double-network hydrogels". In: *Journal of the Mechanics and Physics of Solids* 100 (2017), pp. 103–130.

[83] VA Marichev. "Maximum surface tension and optimum surface electron density". In: *Colloids and Surfaces A: Physicochemical and Engineering Aspects* 389.1-3 (2011), pp. 63–68.

[84] Elaine N. Marieb and Suzanne M. Keller. "Essentials of Human Anatomy & Physiology, 12th Edition". In: Pearson Education, 2017, p. 183. ISBN: 0134395328.

[85] Eric J Markvicka et al. "An autonomously electrically self-healing liquid metal–elastomer composite for robust soft-matter robotics and electronics". In: *Nature materials* (2018), p. 1.

[86] Andrew J McDaid. *Ionic Polymer Metallic Composite Transducers for Biomedical Robotics Applications*. Lulu. com, 2014.

[87] Tissaphern Mirfakhrai, John DW Madden, and Ray H Baughman. "Polymer artificial muscles". In: *Materials today* 10.4 (2007), pp. 30–38.

[88] Aslan Miriyev, Kenneth Stack, and Hod Lipson. "Soft material for soft actuators". In: *Nature communications* 8.1 (2017), p. 596.

[89] Seyed M Mirvakili and Ian W Hunter. "Artificial muscles: Mechanisms, applications, and challenges". In: *Advanced Materials* 30.6 (2018), p. 1704407.

[90] Shuhei Miyashita et al. "An untethered miniature origami robot that self-folds, walks, swims, and degrades". In: *Robotics and Automation (ICRA), 2015 IEEE International Conference on*. IEEE. 2015, pp. 1490–1496.

[91] Volodymyr Mnih et al. "Human-level control through deep reinforcement learning". In: *Nature* 518.7540 (2015), p. 529.

[92] Volodymyr Mnih et al. "Playing atari with deep reinforcement learning". In: *arXiv preprint arXiv:1312.5602* (2013).

[93] Richard M Murray. *A mathematical introduction to robotic manipulation*. CRC press, 2017.

[94] Masaki Nakahata et al. "Redox-generated mechanical motion of a supramolecular polymeric actuator based on host–guest interactions". In: *Angewandte Chemie* 125.22 (2013), pp. 5843–5847.

[95] Sia Nemat-Nasser and Chris W Thomas. "Ionomeric polymer–metal composites". In: *Electroactive Polymer (EAP) Actuators as Artifical Muscles. Reality, Potential, and Challenges, SPIE Press, Washington* (2001).

[96] Philippe Nghe et al. "Microfabricated polyacrylamide devices for the controlled culture of growing cells and developing organisms". In: *PloS one* 8.9 (2013), e75537.

[97] Christian Ohm, Martin Brehmer, and Rudolf Zentel. "Liquid crystalline elastomers as actuators and sensors". In: *Advanced Materials* 22.31 (2010), pp. 3366–3387.

[98] Etienne Palleau et al. "Reversible patterning and actuation of hydrogels by electrically assisted ionoprinting". In: *Nature communications* 4 (2013), p. 2257.

[99] Ke Pan et al. "The performance of a silica-based mixed gel electrolyte in lead acid batteries". In: *Journal of Power Sources* 209 (2012), pp. 262–268.

[100] Ron Pelrine et al. "High-speed electrically actuated elastomers with strain greater than 100%". In: *Science* 287.5454 (2000), pp. 836–839.

[101] Rob Phillips et al. *Physical biology of the cell*. Garland Science, 2012.

[102] Gerald H Pollack. "Cells, gels and mechanics". In: *WIT Transactions on Ecology and the Environment* 73 (2004).

[103] Paul Rea. *Essential clinically applied anatomy of the peripheral Nervous system in the head and neck*. Academic Press, 2016.

[104] MJ Regan et al. "X-ray study of the oxidation of liquid-gallium surfaces". In: *Physical Review B* 55.16 (1997), p. 10786.

[105] Steven I Rich, Robert J Wood, and Carmel Majidi. "Untethered soft robotics". In: *Nature Electronics* 1.2 (2018), p. 102.

[106] Loren Russell, James Wissman, and Carmel Majidi. "Liquid metal actuator driven by electrochemical manipulation of surface tension". In: *Applied Physics Letters* 111.25 (2017), p. 254101.

[107] Thomas BH Schroeder et al. "An electric-eel-inspired soft power source from stacked hydrogels". In: *Nature* 552.7684 (2017), p. 214.

[108] Clarence E Schutt and Uno Lindberg. "A new perspective on muscle contraction". In: *FEBS letters* 325.1-2 (1993), pp. 59–62.

[109] Sangok Seok et al. “Meshworm: a peristaltic soft robot with antagonistic nickel titanium coil actuators”. In: *IEEE/ASME Transactions on mechatronics* 18.5 (2013), pp. 1485–1497.

[110] Virginia A Shepherd. “The cytomatrix as a cooperative system of macromolecular and water networks”. In: *Current topics in developmental biology* 75 (2006), pp. 171–223.

[111] David Silver et al. “Mastering the game of Go with deep neural networks and tree search”. In: *nature* 529.7587 (2016), p. 484.

[112] Aiva Simaite. “Development of ionic electroactive actuators with improved interfacial adhesion: towards the fabrication of inkjet printable artificial muscles”. PhD thesis. Toulouse, INSA, 2015.

[113] Metin Sitti et al. “Biomedical applications of untethered mobile milli/microrobots”. In: *Proceedings of the IEEE* 103.2 (2015), pp. 205–224.

[114] James A Spudich. “The myosin swinging cross-bridge model”. In: *Nature Reviews Molecular Cell Biology* 2.5 (2001), p. 387.

[115] Jeong-Yun Sun et al. “Highly stretchable and tough hydrogels”. In: *Nature* 489.7414 (2012), p. 133.

[116] Richard RA Syms et al. “Surface tension-powered self-assembly of microstructures-the state-of-the-art”. In: *Journal of Microelectromechanical systems* 12.4 (2003), pp. 387–417.

[117] S Tasoglu et al. “Untethered micro-robotic coding of three-dimensional material composition”. In: *Nature communications* 5 (2014), p. 3124.

[118] Benjamin CK Tee et al. "An electrically and mechanically self-healing composite with pressure-and flexion-sensitive properties for electronic skin applications". In: *Nature nanotechnology* 7.12 (2012), p. 825.

[119] Donald L Thomsen et al. "Liquid crystal elastomers with mechanical properties of a muscle". In: *Macromolecules* 34.17 (2001), pp. 5868–5875.

[120] Hongmiao Tian et al. "Polydopamine-Coated Main-Chain Liquid Crystal Elastomer as Optically Driven Artificial Muscle". In: *ACS applied materials & interfaces* 10.9 (2018), pp. 8307–8316.

[121] Paola Tonino et al. "The giant protein titin regulates the length of the striated muscle thick filament". In: *Nature communications* 8.1 (2017), p. 1041.

[122] Melanie G Urbanchek et al. "Specific force deficit in skeletal muscles of old rats is partially explained by the existence of denervated muscle fibers". In: *The Journals of Gerontology Series A: Biological Sciences and Medical Sciences* 56.5 (2001), B191–B197.

[123] Alan S Verkman. "Solute and macromolecule diffusion in cellular aqueous compartments". In: *Trends in biochemical sciences* 27.1 (2002), pp. 27–33.

[124] Hendrik Wermter and Heino Finkelmann. "Liquid crystalline elastomers as artificial muscles". In: *e-Polymers* 1.1 (2001).

[125] James Wissman, Michael D Dickey, and Carmel Majidi. "Field-Controlled Electrical Switch with Liquid Metal". In: *Advanced Science* 4.12 (2017), p. 1700169.

[126] Robert J Wood. "The first takeoff of a biologically inspired at-scale robotic insect". In: *IEEE transactions on robotics* 24.2 (2008), pp. 341–347.

[127] Robert John Wood. "Composite microstructures, microactuators and sensors for biologically inspired micro air vehicles". PhD thesis. University of California, Berkeley, 2004.

[128] Cornell Wright et al. "Design of a modular snake robot". In: *Intelligent Robots and Systems, 2007. IROS 2007. IEEE/RSJ International Conference on*. IEEE. 2007, pp. 2609–2614.

[129] Ping Xie and Rongben Zhang. "Liquid crystal elastomers, networks and gels: advanced smart materials". In: *Journal of Materials Chemistry* 15.26 (2005), pp. 2529–2550.

[130] Qin Xu et al. "Effect of oxidation on the mechanical properties of liquid gallium and eutectic gallium-indium". In: *Physics of Fluids* 24.6 (2012), p. 063101.

[131] Guang-Zhong Yang et al. "The grand challenges of Science Robotics". In: *Science Robotics* 3.14 (2018), eaar7650.

[132] ChangKyu Yoon et al. "Functional stimuli responsive hydrogel devices by self-folding". In: *Smart Materials and Structures* 23.9 (2014), p. 094008.

[133] Yanlei Yu and Tomiki Ikeda. "Soft actuators based on liquid-crystalline elastomers". In: *Angewandte Chemie International Edition* 45.33 (2006), pp. 5416–5418.

[134] Hyunwoo Yuk et al. "Hydraulic hydrogel actuators and robots optically and sonically camouflaged in water". In: *Nature communications* 8 (2017), p. 14230.

[135] Hyunwoo Yuk et al. "Skin-inspired hydrogel–elastomer hybrids with robust interfaces and functional microstructures". In: *Nature communications* 7 (2016), p. 12028.

[136] Yusril Yusuf et al. "Swelling dynamics of liquid crystal elastomers swollen with low molecular weight liquid crystals". In: *Physical Review E* 69.2 (2004), p. 021710.

[137] Qiang Zhao et al. “An instant multi-responsive porous polymer actuator driven by solvent molecule sorption”. In: *Nature communications* 5 (2014), p. 4293.

[138] Ruiqi Zhao et al. “Gas eruption phenomenon happening from Ga-In alloy in NaOH electrolyte”. In: *Applied Physics Letters* 111.24 (2017), p. 241906.

[139] Xuanhe Zhao, Wei Hong, and Zhigang Suo. “Inhomogeneous and anisotropic equilibrium state of a swollen hydrogel containing a hard core”. In: *Applied Physics Letters* 92.5 (2008), p. 051904.

[140] Ma Zhenyi et al. “High field electrostrictive response of polymers”. In: *Journal of Polymer Science Part B: Polymer Physics* 32.16 (1994), pp. 2721–2731.

[141] Longxiang Zhu, Jianhui Qiu, and Eiichi Sakai. “A high modulus hydrogel obtained from hydrogen bond reconstruction and its application in vibration damper”. In: *RSC Advances* 7.69 (2017), pp. 43755–43763.